MASTER THESIS

Thesis submitted in partial fulfillment of the requirements for the degree of Master of Science in Engineering at the University of Applied Sciences Technikum Wien - Degree Program Tissue Engineering and Regenerative Medicine

Plasmonic biosensing with peptide ligands

Submitted by: Vanessa Jungbluth, BSc.
Student number: te16m033

1. Company supervisor: Dr. Jakub Dostálek

   BioSensor Technologies
   AIT Austrian Institute of Technology GmbH
   Konrad-Lorenz-Strasse 24 | 3430 Tulln | Austria

2. FH supervisor: Dr. Heidemarie Fuchs-Eitel

   FH Technikum Wien
   Höchstädtplatz 6 | 1200 Wien | Austria

Tulln, 10th of June, 2018

FH University of Applied Sciences TECHNIKUM WIEN

Declaration of Authenticity

“As author and creator of this work to hand, I confirm with my signature knowledge of the relevant copyright regulations governed by higher education acts (for example see §§ 21, 42f and 57 UrhG (Austrian copyright law) as amended as well as § 14 of the Statute on Studies Act Provisions / Examination Regulations of the UAS Technikum Wien).

In particular I declare that I have made use of third-party content correctly, regardless what form it may have, and I am aware of any consequences I may face on the part of the degree program director if there should be evidence of missing autonomy and independence or evidence of any intent to fraudulently achieve a pass mark for this work (see § 14 para. 1 Statute on Studies Act Provisions / Examination Regulations of the UAS Technikum Wien).

I further declare that up to this date I have not published the work to hand nor have I presented it to another examination board in the same or similar form. I affirm that the version submitted matches the version in the upload tool.”

Place, Date	Signature

Kurzfassung

Die Oberflächenplasmonenresonanzspektroskopie (SPR) stellt eine leistungsfähige Methode dar, um Affinitätswechselwirkungen von großen und mittelgroßen Molekülen zu ihren Bindungspartnern, die an einer festen Oberfläche (typischerweise Gold) haften, zu untersuchen. Die Analyse von Analyten mit niedrigem Molekulargewicht und von Proben mit sehr niedrigen Konzentration bleibt jedoch eine Herausforderung, da die durch Analytbindung induzierte Änderung des Brechungsindex zu gering ist, um gemessen zu werden. Das Ziel dieser Arbeit war es, oberflächenplasmonenverstärkte Fluoreszenzspektroskopie (SPFS) für die Interaktionsanalyse niedermolekularer Peptide, die für die Affinitätsbindung an Integrine entwickelt wurden, zu implementieren. Die Wechselwirkung mit Oberflächenplasmonen kann das gemessene Fluoreszenzsignal in ihrem evaneszenten Feld in der Nähe der metallischen Sensoroberfläche stark erhöhen.

Im ersten Teil dieser Arbeit wurde SPFS für eine biomolekulare Interaktionsstudie verwendet. Integrinrezeptoren ($\alpha_v\beta_3$ und $\alpha_5\beta_1$) wurden auf verschiedenen Oberflächen immobilisiert und dienten als Liganden, verschiedene Peptide dienten als Analyt. Durch unterschiedliche Oberflächenarchitekturen (Thiol-SAM und pNIPAAm-basiertes Hydrogel) konnten Affinitätskonstanten im nM-Bereich für optimierte und neu synthetisierte bicyclische Peptide und Knottin Peptide gemessen werden. Für Kontrollpeptide (cyclische, lineare, negative Kontrolle) konnte keine Bindung beobachtet werden. Es wurde gezeigt, dass SPFS eine nützliche Methode zur Messung der Bindungskinetik ist. Es wurde gezeigt, dass eine Hydrogel Matrix den Vorteil eines stärkeren Fluoreszenzsignals aufgrund des größeren Abstandes von dem Metall bietet, der ein Löschen der Fluoreszenzemission vermeidet.

Im zweiten Teil dieser Arbeit wurde die Hydrogel Matrix zum Nachweis von Biomarkern implementiert, in dem der Assay umgedreht wurde. In diesem Fall wurden Peptide auf der Oberfläche immobilisiert und dienten als Ligand. Ein Antikörper diente als Analyt. Eine SPFS-Studie zeigte die erfolgreiche Etablierung eines Klick-basierten Kopplungsprotokolls und hoher Anti-Fouling-Eigenschaften der Hydrogel-Bindungsmatrix.

Schlagwörter: Oberflächenplasmonenresonanzspektroskopie, Affinitätswechselwirkungen, Dissoziationskonstante K_d, Click-Chemie, Integrin, Hydrogel

Abstract

Surface plasmon resonance (SPR) provides a powerful tool for the observations of affinity interactions of large and medium sized molecules with their ligands attached to solid (typically gold) surface. However, the analysis of low molecular weight analytes and the of samples with very low concentrations of analytes remains a challenge as the measured analyte binding-induced change of the refractive index is too small. The aim of our study was to implement surface plasmon-enhanced fluorescence spectroscopy (SPFS) for the interaction analysis of low molecular weight peptides designed for affinity binding to integrins. The interaction with surface plasmons can greatly increase the measured fluorescence signal within their evanescent field in the close proximity to the metallic sensor surface

In the first part of this thesis, SPFS was used for a biomolecular interaction study. Integrin receptors ($\alpha_v\beta_3$ und $\alpha_5\beta_1$) were immobilized onto different surfaces and served as ligand, various peptides served as analyte. By different surface architectures (thiol-SAM and pNIPAAm based hydrogel) it was possible to measure affinity constants in nM range for optimized and newly synthesized bicyclic peptides and control knottin peptides. For control peptides (cyclic, linear, negative control) no binding could be observed. SPFS was shown to be a useful tool to measure binding kinetics. A hydrogel binding matrix was shown to offer the advantage of stronger fluorescence signal due to the longer distance from the metal which avoids quenching of the fluorescence emission.

In the second part of this thesis, the hydrogel binding matrix was implemented into the detection of biomarkers when the assay was flipped around. In that case, peptides were immobilized on the surface and served as ligand. An antibody served as analyte. A SPFS study revealed the successful establishment of a click-based coupling protocol and high anti-fouling properties of the hydrogel binding matrix.

Keywords: Surface plasmon resonance, affinity interactions, dissociation constant K_d, Click-Chemistry, Integrin, hydrogel

Acknowledgments

At first, the official part. Thanks for the money. This project has received funding from the European Union's Horizon 2020 research and innovation program under grant agreement No 642787, Marie Sklodowska-Curie Innovative Training Network BIOGEL and under Grant agreement No. 633937, project ULTRAPLACAD.

My deepest appreciation goes to my group leader Dr. Jakub Dostalek, for his guidance and for giving me the opportunity to start working within the BST group. After working in night shifts for one semester, this job finally gave me back some sleep and the feeling that my studies lead to something. I learned so much here. Not only about SPR, SPFS and laser intensities. But also, about life. Mostly at all the conferences, summer- and winter schools. I guess at the ASCOS I learned more than in all the previous 25 years of my life. Thank you for sending me there.

Thank you, Heidi, for reviewing my Thesis with a lot of patience and a lot of constructive feedback, even in the last minute.

A big thank you goes to the whole BST group at the AIT for integrating, motivating and supporting me so well. I enjoyed my time with you so much. Stefan and Nestor, thank you for all your technical support and also for the cheering when I was crying and laughing simultaneously again. Anil, you are the Master of Alignment, thanks for all your help! Daria, Hulan, Priya and Simone, you were such an inspiration to me. Meeting you changed me so much. I am very glad that I met such strong people as you. You made me believe in myself. Thank you for always being there.

Thank you to my 'international gang' at the FH. You made my stay in Vienna so much fun. I also would like to thank all the other people at the AIT; spending valuable coffee fresh-air breaks with me.

Finally, I would like to thank my parents, who have always supported me and are so proud at me. I hope that one day, my research can lead to something that improves your life. This is why I started and this is why I will continue. Thank you for the support, trust and motivation.

Content

1. Introduction

1.1 Biosensors

Numerous types of biosensors have been pursued for applications in various fields as food industry for quality and safety checks, in fermentation industry for the detection of glucose concentrations, in medical industry for diagnostic applications and finally in drug discovery [1]. Biosensors became of great importance also in tissue engineering and regenerative medicine, particular in maintaining 3-dimensional (3D) cell cultures and in the development of “organs-on-a-chip” models, where concentrations of biomolecules play an important role in determining the fate of cells and tissues. Monitoring analytes as oxygen, metabolic compounds and proteins can give an insight into cellular activities in real time [2]. Following IUPAC, a biosensor is defined as a self-contained integrated device that is capable of providing specific (semi-)quantitative analytical information using a biological recognition element which is in direct spatial contact with a transduction element [3]. The transducer converts the recognition of an analyte (molecular binding) into a signal [4]. The procedure of a biosensor is illustrated in Figure 1.

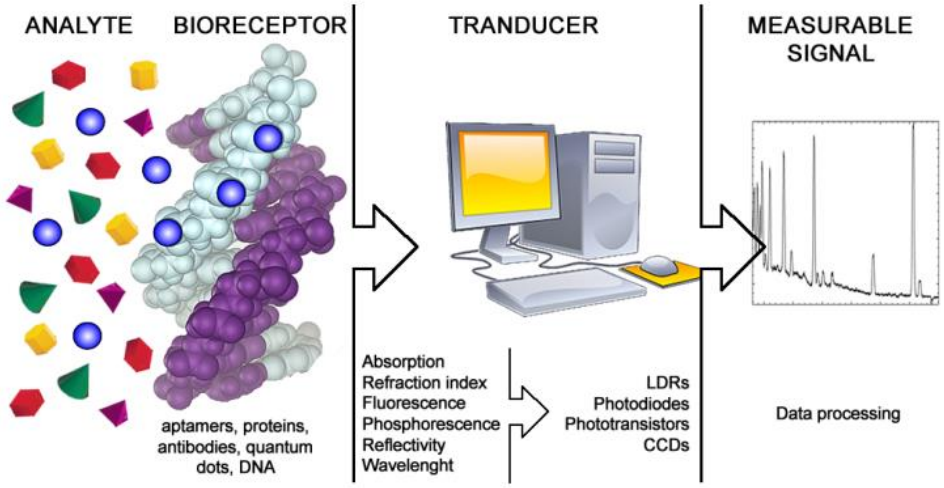

Figure 1: *The components involved in biosensing. An analyte binds to a bioreceptor immobilized to the surface. The bioreceptor can be aptamers, proteins, quantum dots, DNA or else. A transducer is in contact with the bioreceptor, converts the recognition of the analyte into a signal and the data is processed into a measurable signal. Adapted from* [5].

Biosensors can be classified into different groups based on the signal transduction. Electrochemical biosensors directly convert a biological event into an electronic signal allowing the analysis of a biological sample [3]. Piezoelectric biosensors translate a mass change from a chemical adsorption event into a chemical signal [3]. Thermometric biosensors translate the change of heat in a biological reaction into a signal and can therefore be used to monitor the extend of a reaction [6]. Finally, optical biosensors are

based on a detection of changes in properties of light resulting from the analyte binding to a surface [7].

1.2 Surface Plasmon Resonance Biosensors

Surface plasmon resonance (SPR) is a label-free optical method to study biomolecular interactions in real time [8]. Typically, it is based on a Kretschmann configuration, which utilizes a prism and metallic film, usually gold of around 50 nm thickness. Light passes through the prism and reflects at the surface towards a detector. When the light is impinging above a certain (critical) angle, it is reflected completely inside of the prism. This is termed as total internal reflection (TIR). At a certain incident angle, which is called the resonance angle, light is absorbed by the collective oscillations of electron density in the metal film, causing them to resonate and propagate in parallel to the metal surface, which is referred to surface plasmons (SPs). The plasmon oscillation generates an electric field, described as evanescent field, ranging about 100 nm from the boundary between metal surface and sample solution [9] (Figure 2). The actual SPR signal can therefore be explained by the electromagnetic 'coupling' of the incident light with the surface plasmon of the gold layer. Changes in refractive index as a response to biomolecular interactions near a thin metal layer are measured [9].

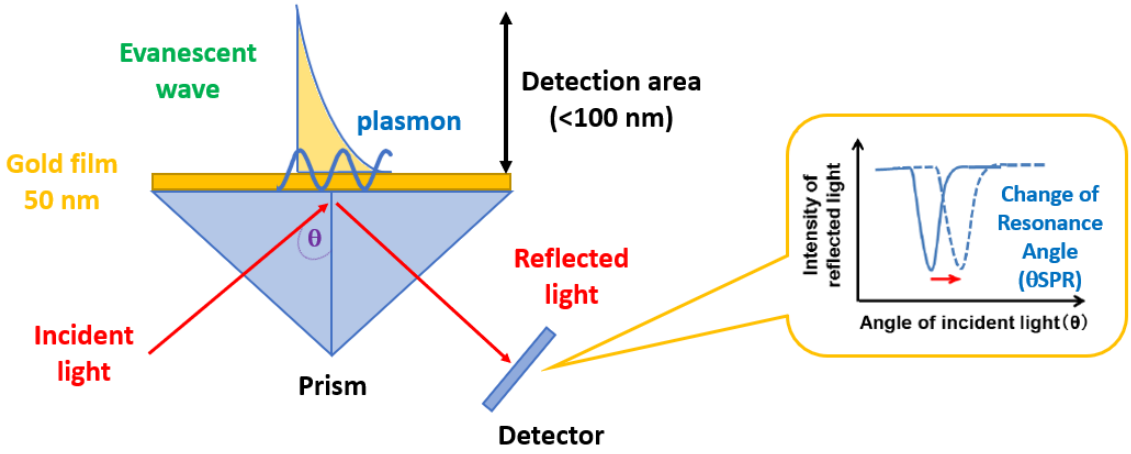

Figure 2: *Principle of SPR. In a Kretschmann configuration, incident light is reflected at a gold film and reflected towards a detector. The light causes surface plasmons, which are oscillating electrons propagating along the surface. Upon binding of molecules to the surface, a shift in refractive index and in the resonance angle can be observed, giving information on surface characteristics* [10], [11]. *Modified from* [11].

Surface plasmons are sensitive to the environment in close proximity to the metal surface. Upon a small change in refractive index of the sensing medium, plasmons cannot be formed. Thus, detection is accomplished by measuring the changes in reflected light

obtained on a detector [12]. A loss in the reflected beam intensity appears as a dip in the SPR reflection intensity curve. The shape and location of this dip can be used to give more information on the sensor surface. If a binding event takes place at the surface, the angular position of the dip shifts and a shift in the reflectivity curve can be observed [12]. This is a direct detection method which avoids the throwbacks of labels. A quantification of surface concentration can be done by monitoring the reflected light intensity or by tracking this shift in resonance angle.

An important aspect of SPR is the observation of time dependent interactions between molecules. In a typical SPR assay, a capturing agent (DNA; antibodies, peptides, etc.) is immobilized on the metal surface. Then a sample solution containing the target molecules is flowed over the surface. The SPR response can be monitored over time at a specific angle by investigating the light intensity. Once molecules bind to the surface, an increase in response can be observed. At some point there will be an equilibrium between binding and unbinding molecules and the response flattens off. After flowing the sample solution, the surface is rinsed with buffer. The binding rate constant k_a can be extracted from the behaviour of the binding response and likewise the dissociation rate k_d can be extracted from the unbinding response. The ratio of these two constants can yield the gradual dissociation constant K_d. In case of no binding events, the response goes back to baseline [13] [14]. The SPR principle is depicted in Figure 3.

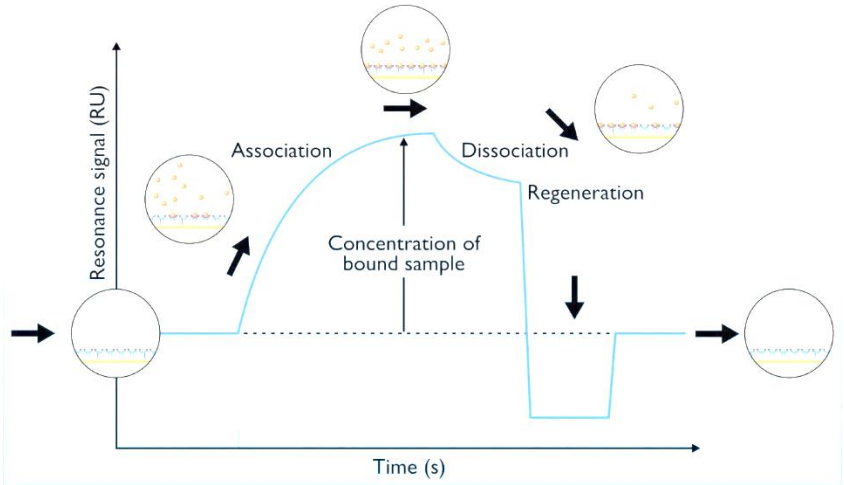

Figure 3: *Sensogram for detecting mass concentration and dissociation changes on the sensor surface via label-free SPR detection* [14]*. Upon binding of molecules to the surface, an increase in response is observed. Once the surface is rinsed with buffer, bound molecules dissociate and the response decreases. In case of no binding of molecules to the surface, the dissociation response goes back to baseline level. A regeneration can be used to remove bound molecules from the surface, so that also this response goes back to baseline.*

The bio-interaction analysis of small molecules with a low molecular weight or with very low concentrations is still a big challenge for the use of SPR. Due to the low weight or concentration of such molecules, the change in refractive index upon binding is below the detection resolution [15].

1.3 Surface Plasmon-Enhanced Fluorescence Spectroscopy Biosensors

In case of insufficient sensitivity of a standard SPR biosensor, surface plasmon enhanced fluorescence spectroscopy (SPFS) biosensors can be applied. This biosensor was firstly introduced in the early 90s by Attridge *et al*. [16] and later simplified by Knoll *et al* [17]. A typical SPFS set up combines the angular modulation of SPR with fluorescence spectroscopy detection (Figure 4). Biomolecular recognition elements for the specific capture of target molecules are bound to a metallic sensor surface [18]. Target molecules contained in a liquid sample are labeled with a fluorophore and flowed over the surface through a flow cell on top of the metallic surface [18]. An excitation laser beam with a wavelength matching the absorption band of the fluorophore conjugated with the target molecules is used to excite molecules bound to the surface [19]. Due to the evanescent field of surface plasmons, fluorescently labeled target molecules in the bulk flow are not excited. The fluorescence light emitted from the surface passes through the flow cell and is collected by a lens. Its intensity is measured by a photomultiplier. A bandpass filter is mounted behind the lens to collect the fluorescence light and to suppress the background signal due to scattering of the excitation light beam. Upon binding of fluorescently labeled target molecules to the sensor surface, a strong peak in the angular fluorescence spectrum is observed and a maximum fluorescence signal occurring upon resonant coupling of surface plasmons can be measured as a function of time enabling the monitoring of kinetics of biomolecular reactions to the sensor surface [20].

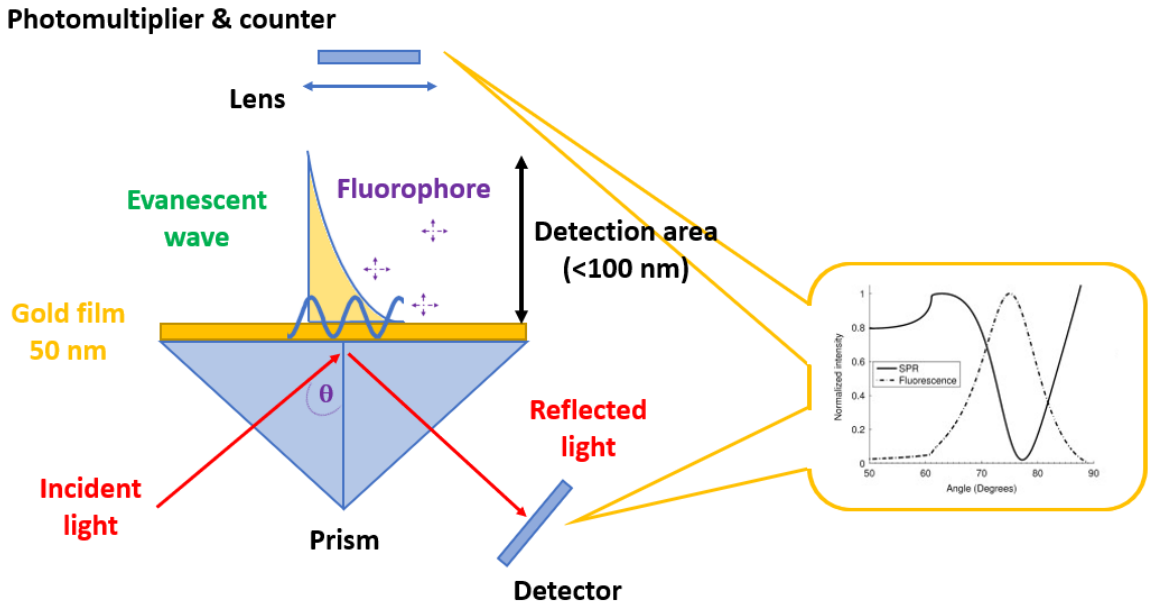

Figure 4: *Optical setup of surface plasmon-enhanced fluorescence spectroscopy (SPFS) utilizing angular modulation of SPR. Target molecules are labelled with a fluorophore and bound molecules close to the metal surface are excited. Fluorescence signal of excited molecules is measured by a photomultiplier. Modified from* [11], [21].

When combing SPFS and SPR, the sensitivity of this method can be further increased. The capturing of fluorophore-labeled molecules to the sensor surface is observed by detecting the emission of fluorescence light from the surface. In this method, the excitation electromagnetic field shows an enhanced intensity when surface plasmons are resonantly excited. The interaction of these surface plasmons increases the measured fluorescence signal intensity as the excitation rate of fluorophores is enhanced by more efficient collecting of fluorescence light. Studies have shown that SPFS-based biosensors allow the analysis of low molecular weight or very low concentrated ligands [22]–[24].

1.4 Interfaces of biosensors

1.4.1 Surface Architecture

The behaviour of a biosensor is strongly influenced by its surface architecture and the immobilized biolayer. This architecture and biolayer are of huge importance for the sensitivity and the detection limits [25]. The coupling procedure chosen to immobilize a ligand to the sensor surface must allow the maintenance of recognising ability [26].

1.4.1.1 Thiol SAM for 2D Surface Architectures

Self-assembled monolayers (SAM) are assemblies formed by the adsorption of constituents from a solution or the gas phase onto a solid surface [27]. The assembly of SAM is usually driven by specific non-covalent interactions as hydrogen-bonding, hydrophobic interactions or van der Waals forces [28]. Head groups of SAMs are bound to

the surface, while the tail groups assemble far from the substrate. The application of SAM determines the choice of head and tail groups [27]. Usually, head groups are connected to a molecular (alkyl) chain in which the terminal end is functionalized by different groups as –OH, -NH2, COOH or –SH groups (Figure 5). Common head groups of SAMs include silanes or thiols, which chemisorb onto a surface, followed by a slow organization of the tail groups. Due to these modifications, wettability and interfacial properties of the layers can be modified [27]. Different ratios of mixed thiols are used to provide specific functionality. Various publications discuss optimal ratios and alkyl chain lengths to provide enough and active binding sites for further modification and to not sterically hinder the binding [27], [29], [30].

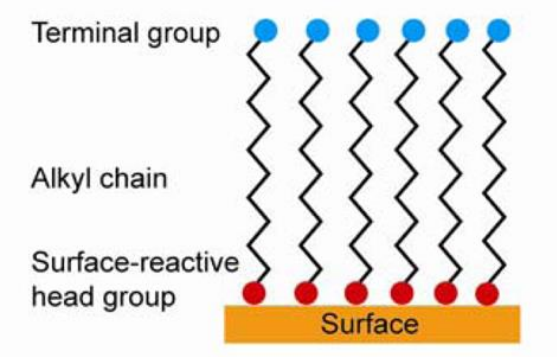

Figure 5: E*xample of a thiol-SAM surface for amine coupling. A SAM is formed by anchoring surface-reactive head groups (for example thiol groups, S) to a surface (for example gold, Au). Head groups and functional terminal groups (for example hydroxy groups, OH) are connected by typically alkyl chains. Modified from* [31]

1.4.1.2 Hydrogels for 3D Surface Architectures

It was shown that a SPFS biosensor does not exhibit the highest sensitivity to biomolecular binding directly at the sensor surface. An optimal distance from the sensor surface to the fluorophore to provide an optimal fluorescent signal was determined as 15-30 nm [20]. At this distance, the quenching of fluorophores and the decay of surface plasmon electromagnetic field intensity are in equilibrium. Therefore, a surface architecture has to provide some spacer of similar thickness. Different approaches have been suggested for that. Polymer brushes are among the most common advanced nanoscale surface modification and can be used to immobilize proteins. They rely on a low protein interaction and a high entropic penalty to provide anti-fouling. A sufficient density of monomers per area is required to achieve these characteristics [20]. Alternatively, hydrogels can be used as 3D polymer networks forming a distance-increasing spacer. Hydrogels are described as hydrophilic, three-dimensional networks that can absorb large quantities of water or other fluids. They are applied in biosensors, in drug delivery vectors and as a carriers or matrices for cells in tissue engineering [32]. For this Master thesis project, a hydrogel derived from

Poly(N-isopropylacrylamide) (pNIPAAm) served as an extended 3D binding matrix. pNIPAAm is a well characterized hydrogel that shows a lower critical solution temperature (LCST) of 32°C. Below this temperature, the hydrogel exhibits a highly open, water swollen structure. Above this temperature the hydrogel collapses with a release of bound water leading to an increase in density and therefore also an increase in refractive index [33], [34]. The structure of a pNIPAAM-based polymer modified with benzophenone is depicted in Figure 6 [34]. The polymer consists of 94 units pNIPAAm, which are causing the thermo-responsiveness, 5 units methacrylic acid, to which a ligand can be covalently immobilized and finally of 1 unit benzophenone methacrylate comonomer to photo crosslink the polymer. Attaching polymer chains covalently to a gold surface can be achieved by photo crosslinking with UV light. The surface is incubated with benzophenone derivatives with a thiol- or disulphide anchor before depositing the hydrogel film.

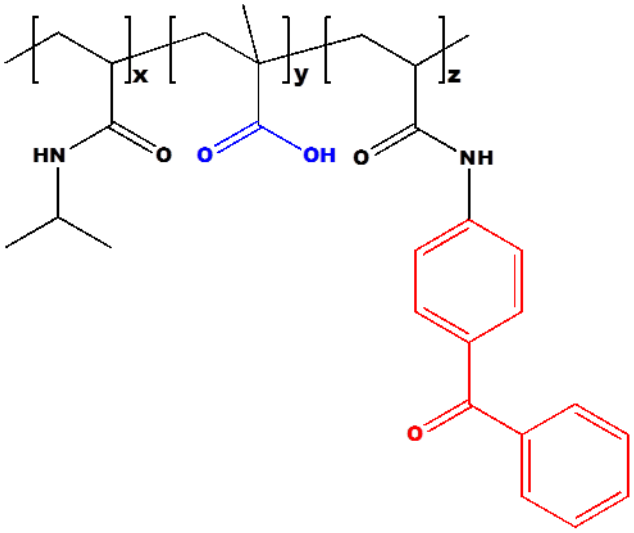

***Figure 6**: Structure of pNIPAAm-based polymer with benzophenone* [34]. *The structure consists of 94 units poly(N-isopropylacrylamide) (indicated in black), 5 units methacrylic acid (indicated in blue) and 1 unit benzophenone methacrylate comonomer (indicated in red).*

1.4.2 Biorecognition Elements

A functional unit that specifically captures an analyte to be detected is described as a biorecognition element. Different biorecognition molecules have been exploited. Usually, they can be divided into two classes: catalytic biorecognition elements like enzymes or affinitive biorecognition elements like antibodies [35]. Enzymes are amino acid based proteins that range in size from less than 100 to more than 2000 amino acid residues [36] When using enzymes as biorecognition elements, many reaction products arise from catalytic processes and can be measured: electrons, protons, heat or light [37]. The enzyme urease is widely used in biosensors for the monitoring of urea in medical and environmental applications. In glucose biosensors the enzyme glucose oxidase is used,

catalysing the oxidation of glucose to gluconolactone [37]. When using antibodies as affinitive biorecognition elements, no target purification is needed before detections as antibodies offer a specific antibody-antigen interaction. For that, the development of monoclonal antibodies by Kohler and Milsteins in 1999 was a big achievement [37]. Aptamers or different types of peptides are other types of biorecognition elements. Aptamers are nucleic acid based ligands isolated form isolated libraries of oligonucleotides by an in vitro selection process called SELEX (Systematic Evolution of Ligands by Exponential enrichment) [38], [39]. Peptide nucleic acid (PNA) based recognition relies on DNA analogues with a polyamide backbone instead of a sugar phosphate backbone [40]. All these biorecognition elements share the high need for a suitable immobilization technique. Different aspects are important for the immobilization of biorecognition elements to a surface. The density of functional groups must be optimized. The more molecules are immobilized, the more analyte is captured. However, if the density of immobilized biomolecules is too high, the analyte cannot reach the binding molecules. Furthermore, on the one hand the target needs a good accessibility, on the other hand, if the spacer is too long it might bend towards the surface and thus will not be accessible. In general, a low non-specific binding and a stable linkage between the biomolecules and the solid support should be achieved [35]. A wide range of immobilization techniques is available, here amine coupling for the covalent immobilization of a biorecognition molecule and a click chemistry-based coupling procedure are emphasized. Other techniques can rely on biotin-avidin interactions, affinity tags or site-specific binding [41].

1.4.2.1 Amine Coupling

Amine coupling is an established technique for covalent immobilization that makes use of the N-terminal and ε-amino groups of a ligands lysine residues, the thiol group of cysteine or carboxylic groups of aspartic and glutamic acids. These groups are bound to free carboxyl or amino groups on a surface using EDC/NHS chemistry [41] (Figure 7). In the first step of this reaction, ethyl(dimethylaminopropyl) carbodiimide (EDC) reacts with a functional group discussed above. This creates an unstable O-acetyl isourea intermediate. *N*-Hydroxysuccinimid *(*NHS) is added to avoid hydrolysis of this product. Hereby, a stable NHS ester is formed and a soluble by-product is released. Instead of NHS, also Sodium para-tetrafluorophenol-sulfonate (TFPS) can be used [42]. This coupling procedure is considered as a strong immobilization in a site-specific orientation.

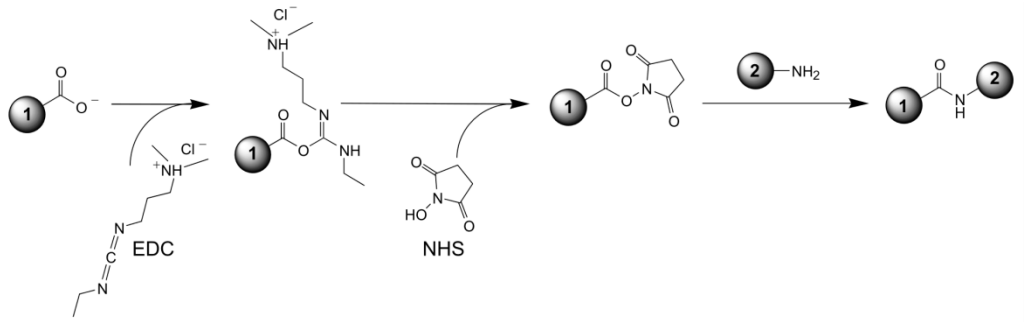

Figure 7: *Principle of EDC/NHS chemistry. Ethyl(dimethylaminopropyl) carbodiimide (EDC) reacts with a carboxyl group of the molecule to be immobilized. Unstable O-acetyl isourea is formed. N-Hydroxysuccinimid (NHS) is added to avoid hydrolysis of this product. Hereby, a stable NHS ester is formed and a soluble by-product is released.*

1.4.2.2 Click Chemistry Based Coupling

The term click chemistry was firstly introduced in 2001 by Sharpless *et al*. [43]. The publication described click chemistry as a chemical philosophy that can generate substances quickly and reliably by joining small units together with high thermodynamic force. According to Sharpless, the requirements for this reaction must be modular, wide in scope, achieve a high yield of product, generate only inoffensive or no by-products, must be stereo specific and have a high atom economy [43]. Additionally. the process must have simple reaction conditions, readily available starting materials and reagents and simple product isolation by non-chromatographic methods [43]. Since introducing this term, click chemistry has a tremendous impact in bioconjugation, material science and drug discovery. Different classes of click reactions have been reported on: cycloaddition reactions, nucleophilic opening of highly strained rings, non-aldol type carbonyl chemistry and reactions of alkenes and alkynes [44], [45]. Copper catalysed alkyne azide cycloaddition (CuAAC), also called Huisgen cycloaddition, is considered as the perfect click reaction. In this reaction a 1,3-dipolar cycloaddition occurs between an azide and a terminal or internal alkyne and a 12,3-triazole is formed [46].

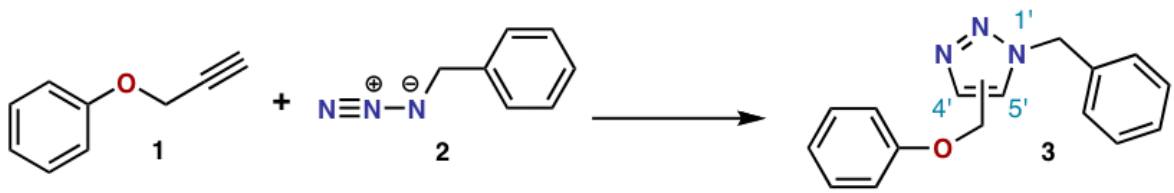

Figure 8: *Principle of the Huisgen cycloaddition. An azide (2) reacts with an alkyne (1) to form a triazole (3) as a mixture of 1,4-adduct and 1,5-adduct.*

1.5 Integrin and Integrin-Binders

1.5.1 Integrin

Integrin is a transmembrane receptor anchored in the cell membrane. It is present in all eukaryotic cells with exception for red blood cells. The heterodimer structure is composed of two connected glycoprotein chains (alpha and beta chain). Integrin facilitates the cell-to-cell or the cell-to-extracellular matrix (ECM) adhesion via an extracellular transmembrane protein domain and an arginine-glycine-aspartic acid (RGD) recognition sign as found in ECM protein ligands (fibronectin in fibroblasts, fibrinogen, van Willebrand factor, vitronectin). Upon adhesion, pathways involved in the cell cycle, in the organization of the intracellular cytoskeleton and in the movement of new receptors on the cell membrane are activated [47] (Figure 9).

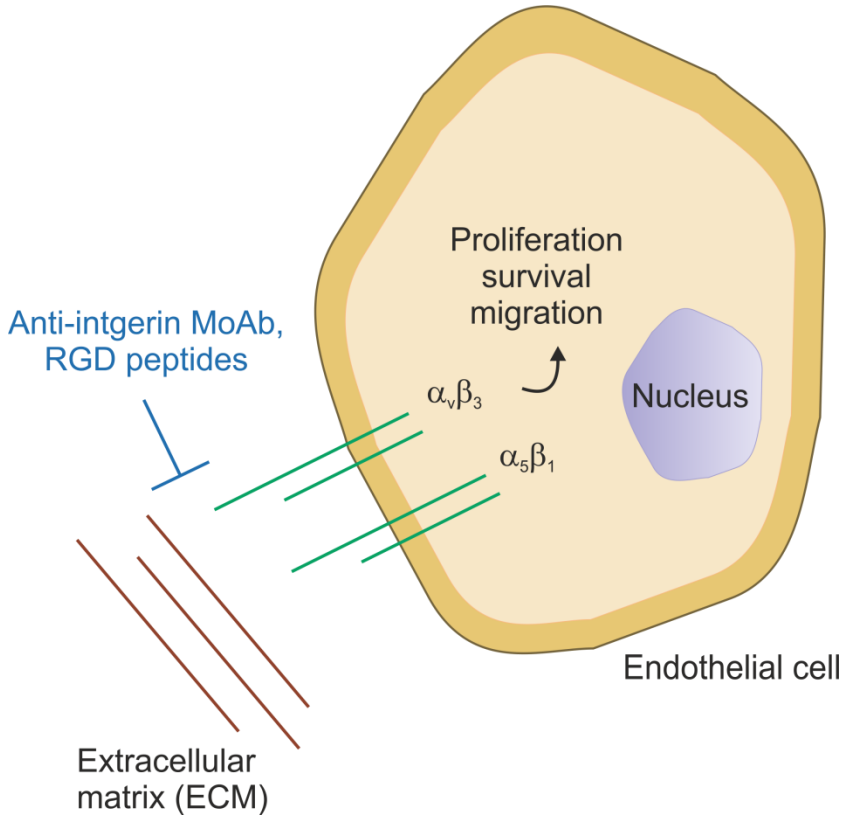

Figure 9: *Different integrin transmembrane receptors ($\alpha_v\beta_3$ and $\alpha_5\beta_1$) located on an endothelial cell membrane. Due to different alpha and beta subunit, different classes of integrin receptors exist. Integrin binds to ECM domains (typically RGD domains) of other cells or of the ECM itself. Upon adhesion, different pathways can be stimulated. Binding can be inhibited by anti-integrin monoclonal antibodies (Anti-integrin MoAb) or by RGD peptides. Modified from* [48].

Several integrins as $\alpha_v\beta_3$ and $\alpha_5\beta_1$ have been shown to be overexpressed on the surface of cancer cells [49]. Integrin $\alpha_v\beta_3$ plays an important role in tumor cell invasion, angiogenesis,

and phagocytosis of apoptotic cells [50]. It is widely expressed on blood vessels of human tumor cells, but no on vessels of normal tissue. Integrin $\alpha_5\beta_1$ mediates cell adhesion and migration by recognition of fibronectin and provides proliferative signals to vascular cells [51]. The disease progression of various tumor types correlates with the expression of several integrin receptors as $\alpha_v\beta_3$, $\alpha_v\beta_5$, $\alpha_5\beta_1$, $\alpha_6\beta_4$, $\alpha_4\beta_1$ and $\alpha_v\beta_6$. Therefore, these are the most studied integrins in cancer [49]. Therefore, in the medical field, there is a high need for integrin-binding species. Among these, peptides are promising integrin-binders. These peptides are supposed to mimic small ECM domains so that they could be used for imaging or for the treatment of cancer. As molecular imaging agents these peptides could detect integrin surface receptors on cancer cells [52]. In cancer treatment these peptides could target integrin surface receptors on cancer cells and block their function [53]. Additionally, integrin-binding peptides could be used to functionalize synthetic materials to improve cellular adhesion [54]. For all these applications, the previously described RGD sequence is of great importance, illustrated in Figure 10.

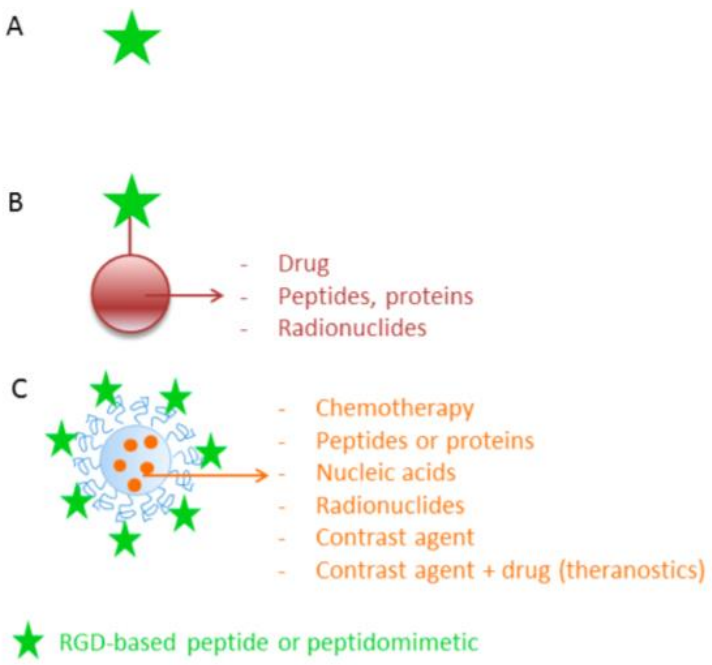

Figure 10: *RGD-based strategies. (A) RGD antagonists. (B) RGD conjugates. The RGD-based peptide or peptidomimetic is conjugated to drugs or radionuclides with covalent links. (C) RGD peptides or peptidomimetics are grafted at the nanoparticle surface (polymeric nanoparticles, liposomes, polymeric micelles, etc.). These structures contains various agents such as anticancer drugs, peptides or proteins, nucleic acids, radionuclides, contrast agents, or a mixture of contrast agents and anticancer drugs (theranostics)* [55].

1.5.2 Integrin Binding Peptides

Different peptide structures have been introduced as integrin binders. Promising candidates for drug development are knottin peptides. In 2016, Cochran *et al*. firstly described cysteine-knot RGD peptides as integrin binders [56]. These knottin peptides consist of a structure with three highly woven disulphide bridges forming a knot (Figure 11). This knot leads to a very high thermal and proteolytic stability.

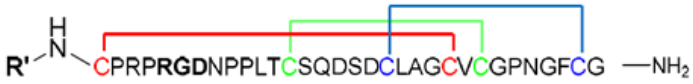

Figure 11: *Structure of knottin peptides. Knottin peptides are composed of three cystein disulphide bridges, one (indicated in green) is passing through the two others (indicated in red and blue), creating a knot* [57].

However, these peptides have a low integrin selectivity, which could cause severe side effects of peptide-based drugs. Additionally, the production of knottin peptides is restricted to natural amino acids, which makes it barely possible to modify them with any functional group. Cyclic peptides offer the advantage of a conformational restriction and a low toxicity, what allows an application for drug development. However, also the synthesis and modification of these peptides is difficult. Bernhagen *et al.* are now reporting on low molecular weight bicyclic peptides with a molecular weight of less than two kilo Dalton (kD) [not published yet]. The bicyclic peptide motif contains the well-known RGD sequence that providing the basic integrin affinity, and the second motif contains a random-diversity sequence which is intended to provide integrin-selectivity. The motifs are enclosed by cysteines, which allows for the double CLIPS-cyclization (Chemical Linkage of Peptides onto Scaffolds), and hence the formation of a bicyclic peptide that comprises two loops [not published yet]. This makes these peptides more proteolytic stable and more affine and selective for their target. Furthermore, these peptides can be easily produced by solid-phase peptide synthesis and can easily be modified with any functional group [not published yet]. The structures of described peptides are depicted in Figure 12.

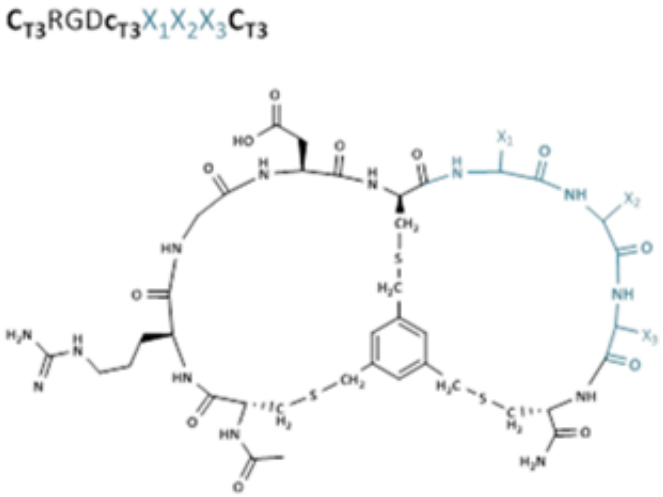

Figure 12: *Structure of bicyclic peptides. Bicyclic peptides are composed of two loops, one with an integrin-binding RGD sequence (indicated in black) providing basic integrin affinity and one with a randomized sequence (indicated in blue) providing integrin selectivity. The motifs are enclosed by cysteines, allowing a CLIPS cyclization (Chemical Linkage of Peptides onto Scaffolds) [not published yet].*

1.5.3 Competitive ELISA for Identifying Potential Integrin Binders

The evaluation of binding affinities between integrin and peptides is a key step to find selective integrin binders. Different assays have been established to evaluate the binding affinities of potential integrin binders. However, these methods are typically not suitable for the screening of large compound libraries. Antibodies, integrin expressing cells or other ECM proteins are required for such assays, which make them expensive and difficult to set up. Bernhagen *et al*. have recently described a new method to investigate the affinity binding of peptides to integrin (Figure 13). They report on a competition ELISA, in which they coat plates with integrin and add a biotinylated knottin-RGD peptide. Studies reported on a very high affinity of this knottin peptide to the previously described integrin receptors $\alpha_v\beta_3$ and $\alpha_5\beta_1$, which are mainly expressed on cancer cells. Binding of this peptide to the integrin is inhibited by adding different concentrations of newly developed peptides or different reference peptides, whose affinity is to be screened. Once streptavidin-peroxidase is added, a colour change is induced. A strong colour change indicates that more biotinylated knottin-RGD peptide was bound and a weak inhibition of this binding occurred. A weak colour change indicates a strong inhibition, as less biotinylated knottin-RGD peptide was bound. When measuring the absorbance of these reactions, a IC50 value can be determined and indicate the inhibition rate of biotinylated knottin-RGD peptide [57].

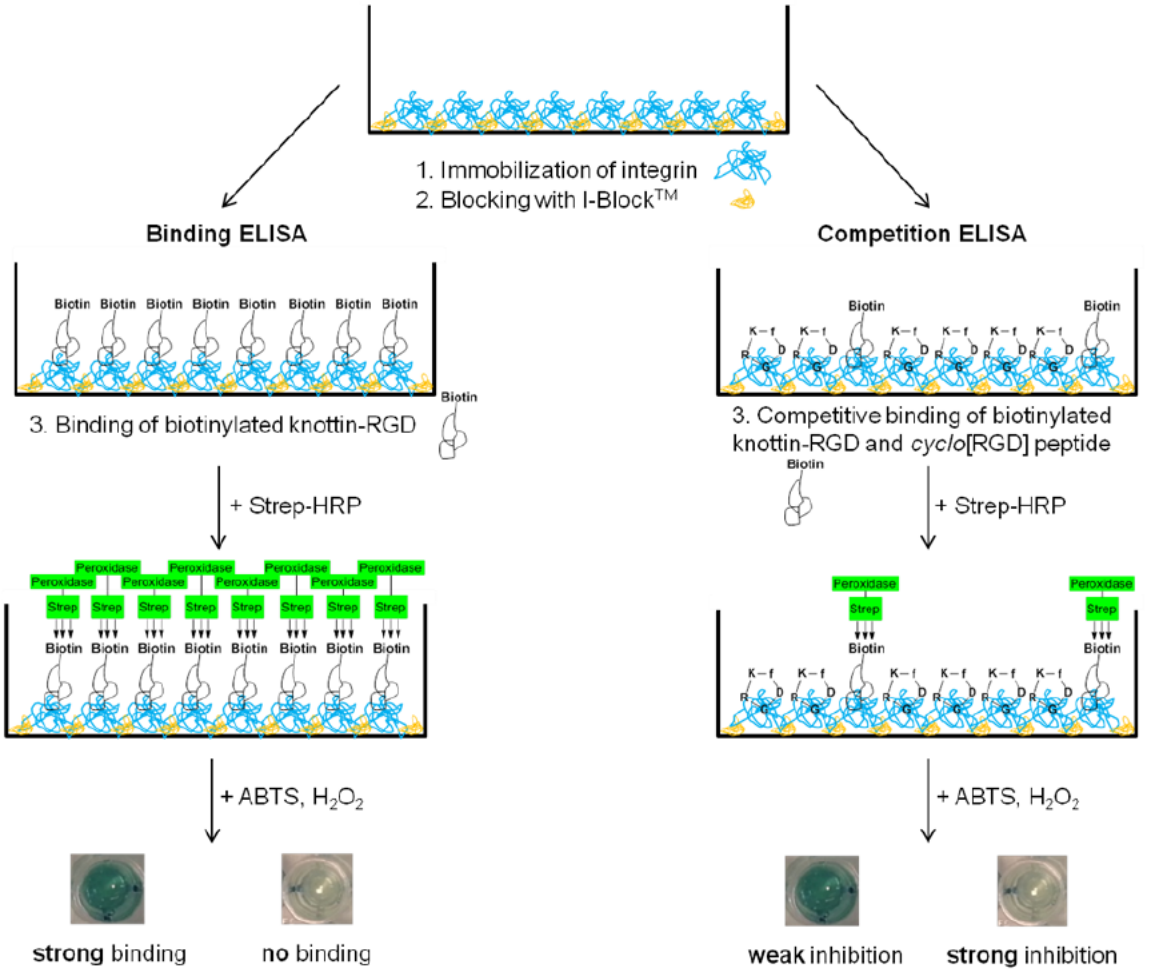

Figure 13: *Schematic setup of the direct binding ELISA (left) and competition ELISA (right). Plates are coated with integrin. Biotinylated-knottin-RGD peptide and different concentrations of the peptide of interest are added. Colour change is induced by biotin-bound streptavidin-horseradish peroxidase ("Peroxidase-Strep"). Only if the binding affinity of the peptide of interest is weak, the biotinylated knottin-RGD peptide will bind to the surface and will not be washed off. The colour change reaction can occur and a strong colour changes indicates a weak inhibition of this peptide binding to the surface* [57].

Despite the fact that this method is a cheap and easy-to-use approach to investigate the affinity binding of new integrin binders, it is still an indirect method. A direct method allowing the measurement of K_d values is needed to validate the results. For such studies, biosensors can be used.

2 Aims

Surface plasmon resonance (SPR) provides a powerful tool for the observations of affinity interactions of large and medium sized molecules with their ligands attached to a solid (typically gold) surface. However, the analysis of low molecular weight analytes and of samples with very low concentrations of analytes remains a challenge as the measured analyte binding-induced change at in refractive index is too small to be detected. Surface plasmon enhanced fluorescence spectroscopy (SPFS) offers means to overcome this problem, as the capture of fluorophore-labelled molecules to the surface can be observed via the detection of amplified fluorescence light emitted from the surface. This technique takes advantage of the enhanced intensity of electromagnetic field accompanied with the resonant excitation of surface plasmons. The interaction with surface plasmons can greatly increase the measured fluorescence signal within their evanescent field in the close proximity to the metallic sensor surface.

The aim of this thesis is to implement the method of SPFS for an interaction analysis of low molecular weight peptides (designed by collaboration partner Pepscan; ~ 2 kDa) designed for affinity binding to integrin transmembrane proteins (~150 kDa). Different surface architectures will be implemented to increase signal intensity due to longer distances of target molecules from the metal which avoids quenching of the fluorescence emission. Immobilization of integrin to these surfaces will be carried out be standard amine coupling and a titration of different target peptide concentrations will be performed to establish a dose response curve and to obtain affinity constants that will be compared to IC_{50} values obtained by a competition ELISA test within the laboratory of collaboration partner Pepscan. Additionally, we want to implement this method to establish a click chemistry coupling based protocol for the immobilization of ligands to the sensor surface. A sandwich assay shall be performed to investigate affinity binding to this ligand.

3 Materials and Methods

3.1 Materials

Table 1: *List of materials.*

Material	Supplier
(3-thiopropyl)oxybenzophenone (BP-thiol)	Synthesized by Prof. Jonas group at University of Siegen [58].
Acetic acid	Sigma-Aldrich (Steinheim, Germany)
Alexa Fluor 647 anti-mouse IgG (A-21236)	Thermo Fisher Scientific (Waltham, USA)
Anti-CA12 mAB (AMAb90639)	Atlas Antibodies (Bromma, Sweden)
$CaCl_2 \cdot 2H_2O$	Merck (Darmstadt, Germany)
CA12 peptide	JPT Peptide Technologies (Berlin, Germany)
Dithiolaromatic PEG3 (thiolPEG; SPT-0013)	SensoPath Technologies (Bozeman, USA)
Dithiolaromatic PEG6-carboxylate (thiol-COOH; SPT0014A6)	SensoPath Technologies (Bozeman, USA)
Ethanolamine	Sigma-Aldrich (Steinheim, Germany)
Ethyl(dimethylaminopropyl) carbodiimide (EDC)	Sigma-Aldrich (Steinheim, Germany)
IgG from mouse serum (I5381)	Sigma-Aldrich (Steinheim, Germany)
$MgCl_2 \cdot 6H_2O$	Merck (Darmstadt, Germany)
$MnCl_2 \cdot 4H_2O$	Sigma-Aldrich (Steinheim, Germany)
N-Hydroxysuccinimide (NHS)	Sigma-Aldrich (Steinheim, Germany)
Phosphate buffered saline (PBS)	Merck (Darmstadt, Germany)
Poly(N-isopropylacrylamide) based terpolymer with 94:5:1 molar ratio of N-isopropylacrylamide, methacrylic acid and 4-methacryloyloxy benzophenone (pNIPAAm)	Synthesized by Prof. Jonas group at University of Siegen (Siegen, Germany) [59]
Recombinant human integrin	R&D Systems (Minneapolis, USA)
S-3-(benzoylphenoxy)propyl ethanthioate (thiol-benzophenone)	Synthesized byProf. Jonas group at University of Siegen (Siegen, Germany) [59]
Sodium acetate	Sigma-Aldrich (Steinheim, Germany)
Sodium para-tetrafluorophenol-sulfonate (TFPS)	Synthesized by Max Planck Institute for Polymer Research (Mainz, Germany) [42],

	[58]
TP53 peptide	JPT Peptide Technologies (Berlin, Germany)
Tween-20	Sigma-Aldrich (Steinheim, Germany)

Table 2: *List of devices.*

Device	Supplier
Counter (53131A)	Agilent (Santa Clara, USA)
Fluorescence band pass filter (670FS10-25)	Andover Corporation Optical Filter (Salem, USA)
Laser notch filter (XNF-632.8-25.0M)	CVI Melles Griot (Albuquerque, USA)
Lockin amplifier	EG&G (Gaithersburg, USA)
Photomultiplier (H6240-01)	Hamamatsu Photonics (Hamamatsu, Japan)
Thermal vacuum evaporation (HHV AUTO 306)	HHV LTD (Crawley, UK)
UV lamp Bio-Link 365	Vilber Lourmat (Eberhardzell, Germany)

3.2 Methods

3.2.1 Optical Setups

An optical system combining surface plasmon resonance (SPR) and surface plasmon enhanced fluorescence spectroscopy (SPFS) was used for direct investigation of affinity interaction of selected peptides and integrin receptors. The Kretschmann configuration of attenuated total reflection method was used for the resonant excitation and interrogation of surface plasmons as described before in more detail [21]. Briefly, a laser beam at wavelength of 633 nm was coupled to a high refractive index glass prism and glass substrate coated with SPR-active thin gold film was optically matched to its base. The beam was made incident at the angle of incidence that was tuned close to θ_{SPR} where surface plasmons are resonantly excited at the outer interface of gold surface.

A flow cell was clamped against the gold sensor surface in order to flow liquid samples with a flow rate of 40 µL/min. The reflected beam intensity was measured with a lockin amplifier in order to track changes in the SPR signal. The fluorescence signal excited via surface plasmons that was propagating from the sensor surface through the flow cell was collected by a lens with a numerical aperture about NA=2 and detected by a photomultiplier (H6240-01, Hamamatsu, Japan) connected to a counter. The intensity of the excitation beam irradiating area on the sensor chip of about mm^2 was reduced to 30-60 µW to decrease

bleaching of Cy5 excited by the enhanced field intensity of surface plasmons. The fluorescence light emitted by Cy5 at a wavelength of about 670 nm was spectrally separated from the excitation light at 633 nm by using a set of laser notch filter and fluorescence band pass filter.

3.2.2 Preparation of Sensor Chips

3.2.2.1 Gold Layer Deposition

Sensor chips were prepared from cleaned BK7 glass substrates which were subsequently coated with metals by thermal vacuum evaporation. In this thin film deposition method, a vacuum is used to coat objects with pure materials in nm to µm range. A 2 nm thin underlying layer of chromium (Cr) was used to prevent the delamination of the 50 nm thick gold (Au) layer, which was used to support the plasmon modes.

3.2.2.2 Preparation of SAMs

The 2D architecture relied on mixed self-assembled monolayer (SAM) that was formed by immersing the gold surface overnight in a 1 mM ethanolic solution with a dithiol-PEG6-COOH and dithiol-PEG3 mixed at molar ratio of 1:9. Afterwards, the gold surface was rinsed with ethanol, dried in a stream of air, and stored under argon atmosphere.

3.2.2.3 Preparation of Hydrogel Layer

In order to obtain a 3D architecture, a protocol for preparation of a thin hydrogel from poly(N)isopropylacrylamide – based polymer was adopted based on our previous work [60]. Briefly, a thin hydrogel film was spin-coated (from an ethanol solution with polymer dissolved at a concentration of 0.5% w/w) on the gold surface, which was modified by a thiol-benzophenone SAM. The polymer film was dried overnight at 50 °C under vacuum and the polymer chains were crosslinked to the gold surface via benzophenone units by irradiating the sample with UV light at λ = 365 nm with an irradiation dose of 2-4 Jcm^2. Afterwards, the gold surface was rinsed with ethanol, dried in a stream of air, and stored under argon atmosphere.

3.2.3 Assay Performance

3.2.3.1 Immobilization of Ligand

The immobilization of integrin $\alpha_V\beta_3$ and $\alpha_1\beta_5$ was performed in situ by amine coupling. The surface reactions were monitored by SPR. Firstly, PBS and acetate buffer with pH=5 were flowed over the gold surface to reach a stable baseline in SPR signal. Then, the sensor surface carrying carboxylic groups on mixed thiol SAM layer was reacted with 75 mg/mL EDC and 21 mg/mL NHS dissolved in water for 15 minutes. For the 3D hydrogel interface, the activation was performed by 75 mg/mL EDC and 21 mg/mL TFPS dissolved in water. Acetate buffer with pH=4 was used to dilute recombinant human integrin $\alpha_5\beta_1$ or $\alpha_V\beta_3$ to a

concentration of 10 µg/mL solution. This solution was flowed over the activated sensor surface for 90 minutes to bind the integrin molecules via their amine groups to activated carboxylic groups. Finally, remaining active ester groups were inactivated by flowing 1 M ethanolamine solution over the gold surface for 15 minutes.

3.2.3.2 Titration Assay

To observe affinity binding of Cy5-labeled peptides to immobilized integrin ligands, PBS with 1 mM $CaCl_2$, 0.5 mM $MnCl_2$, 1 mg/mL BSA and 0.05% Tween-20 was used as running buffer. The peptide was diluted at concentration of c=0.1, 1, 5, 10, 50, 100, and 1000 nM and sequentially flowed over the sensor surface. Each concentration was allowed to react with the integrin for 30 minutes followed by rinsing the surface with running buffer solution for 10 minutes. The affinity binding of target analyte was monitored in real-time by measuring the fluorescence intensity F(t) originating from the close proximity to the sensor surface that was probed by resonantly excited surface plasmons. The fluorescence signal F gradually increases upon the affinity binding of target analyte and for each concentration, the equilibrium fluorescence signal ΔF was determined as a difference between fluorescence baseline and after 10 min rising with running-buffer.
The titration curve was established based on these values and it was fitted with a Langmuir isotherm model as illustrated in Equation 1 in order to determine the equilibrium dissociation constant K_d.

Equation 1: *Formula for a Langmuir isotherm model.*

$$\Delta F(c) = \frac{\Delta Fmax * c}{Kd + c}$$

3.2.3.3 Immobilization by Click-Based Coupling

A 2.5% w/w pNIPAAM based hydrogel 3D surface architecture was prepared as described before (chapter 3.2.2.3). Carboxyl groups in the hydrogel were activated using EDC/TFPS (21/75 mg/mL respectively) in water for 15 minutes. After washing with ACT buffer pH 5, 2.6 µM amine-azide in ACT buffer pH 5 reacted with the hydrogel for 1 hour. After rinsing with water, unreacted groups were passivated for 15 minutes with 1M ethanolamine pH 8.5 in water. The click coupling of peptides with alkyne moieties into the hydrogel with azide groups was performed outside the flow cell (ex situ) (Figure 14).

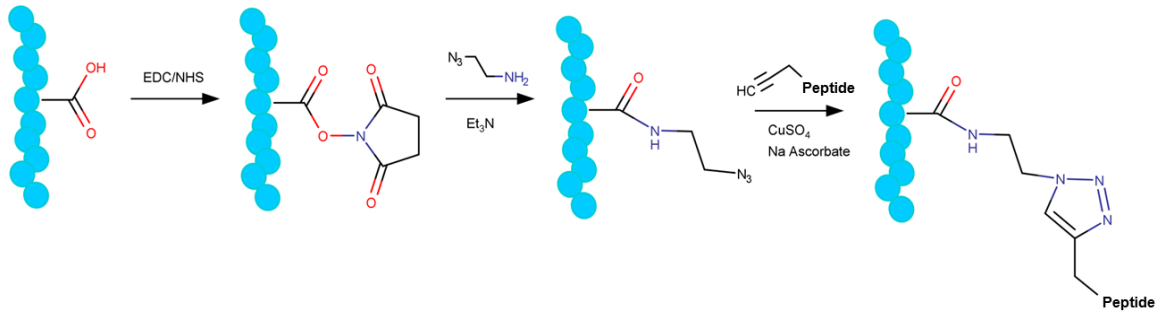

Figure 14: *Schematics of amine coupling of amine azide to a pNIPAAm-based hydrogel followed by a click-based coupling of peptide.*

A solution of 0.05 M $CuSO_4$* $5H_2O$ in 3:1 DMSO/t-butanol and a solution of 0.05 M TBTA in 3:1 DMSO/t-butanol was mixed 1:2. To 1.5 µL of this solution 0.75 µl 0.1 M Na-ascorbate in water were added, as well as 2 µL of the peptide which was dissolved in PBS. 4.38 µL DMSO and 1.37 µl H_2O were added to a final volume of 10 µL. All reagents were freshly prepared. A volume of 7.5 µL was pipetted onto the sensor chip, covered with a cover slit and let reacted for 2 hours in the dark. Afterwards, 1 µl of 50 µg/mL carboxybetaine alkyne in H_2O was added to the sensor chip and incubated for 15 minutes in the dark. Finally, the chip was rinsed with water and PBS with 1 mg/mL BSA and 0.05% Tween (PBST+BSA) and put back into the set-up, where it was washed with PBST+BSA for one more hour.

In this study, CA12 was chosen as a model peptide to validate functionality of the click-based coupling protocol. CA12 has been described for cancer diagnostics [61]. The peptide sequence of HLQHVKYKGQEAFVP has a molecular weight of about 2.5 kDa, an isoelectric point above 9 and can affinity-bind to the monoclonal mouse antibody a-CA12 [61]. For a control experiment, the protein TP53 was chosen. TP53 has been described as an a tumor suppressor [62] with a sequence of EYFTLQIRGRERFEM and cannot affinity-bind to the monoclonal mouse antibody a-CA12. Therefore, it was chosen as a control peptide. Both peptides were modified with an alkyne tag at their N terminus with a PEG spacer.

To investigate the affinity binding of a-CA12 antibody to the click-immobilized peptide, a SPFS study was performed. After the surface preparation, CA12 ligand or TP53 as a control ligand were click-immobilized. SPFS signal angular scans were measured after a sequential flow of samples (PBS spiked with mouse a-CA12 at concentration of 10, 100, and 1000 ng/mL for 30 minutes) followed by the flow of detection a-mIgG antibody labelled with Alexa Fluor 647 (2 µg/mL for 30 minutes) after 10 minutes of rinsing with buffer. The fluorescence response for each a-CA12 concentration was determined as a difference in the fluorescence intensity ΔF prior to the injection of a-CA12 and after the subsequent flow

of a-mIgG-Alexa Fluor 647 and rinsing with buffer. From this calibration curve, enhanced fluorescence signal intensity could be seen in the specific binding reaction.

4 Results

4.1 Peptide Integrin Interaction Study on Thiol-SAM Surface

The interaction of a bicyclic-RGD peptides optimized for $\alpha_V\beta_3$ (clips-PS48) and for $\alpha_5\beta_1$ (clips-TEC213) is compared to the interaction of knottin-RGD (knottin-TEC205), cyclic-RGD peptides (PS51) and linear peptides. (TEC218). For a better understanding of peptide names and their binding partner, a summary is depicted in Table 3.

Table 3: *Names and potential binding partner of peptides used in this study.*

Peptide		Potential binding partner
Bicyclic peptide optimized for $\alpha_v\beta_3$	clips-PS48	$\alpha_v\beta_3$
Bicyclic peptide optimized for $\alpha_5\beta_1$	clips-TEC213	$\alpha_5\beta_1$
Knottin peptide	knottin-TEC205	$\alpha_v\beta_3$, $\alpha_5\beta_1$
Cyclic peptide	PS51	$\alpha_v\beta_3$, $\alpha_5\beta_1$
Linear peptide	TEC218	none (control)

A 2D surface architecture based on a thiol-SAM (Figure 15) was used to covalently immobilize integrin to the surface (Figure 16). A titration of different fluorescently labelled peptide concentrations was performed (Figure 17) to obtain a dose response curve to be used for a Langmuir fit to obtain the K_d of integrin-peptide interactions.

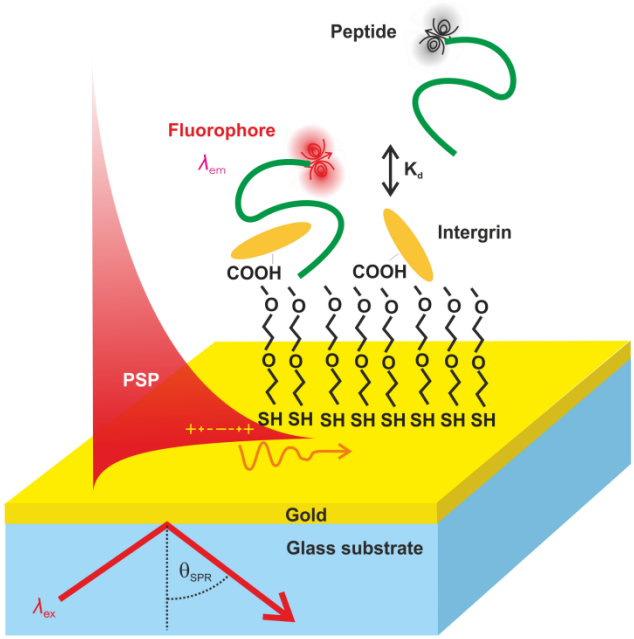

Figure 15: *2D surface architecture based on a thiol-self-assembled-monolayer (SAM). In the Kretschmann configuration, a gold film is attached to a glass substrate. For the establishment of a 2D architecture (relying on mixed thiol-SAM of a 1.9 molar ratio mixture of dithiol-PEG6-COOH and dithiol-PEG3), thiol head groups (SH) are anchored to the gold surface. Terminal carboxyl groups (COOH) of the dithiol are used to covalently bind integrin to the SAM layer. Cy5 labelled peptide binds to integrin. The binding is probed at a certain incident angle (θ_{SPR}), at which the light is coupled to electrons in the dielectric interface. Surface plasmons are created and propagate along the surface (therefore called propagating surface plasmons, PSP). The dissociation constant K_d of a peptide binding to immobilized integrin can be investigated.*

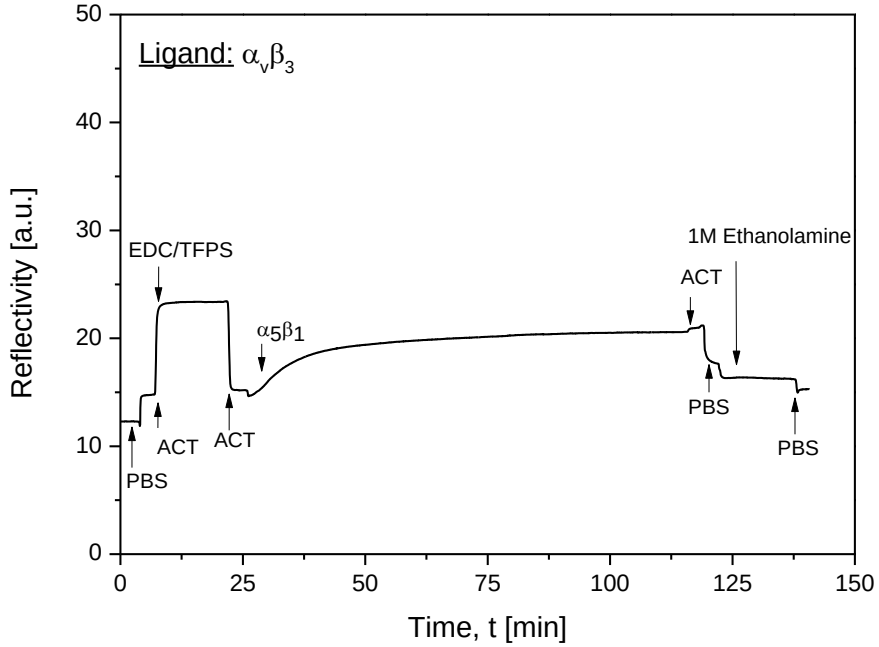

Figure 16: *Sensorgram of immobilization on thiol-SAM surface. Carboxyl groups of the surface are activated via EDC/TFPS chemistry. Integrin is covalently bound to these groups. Remaining functional groups are blocked with 1 M Ethanolamine. An increase in reflectivity is observed upon binding of molecules to the surface.*

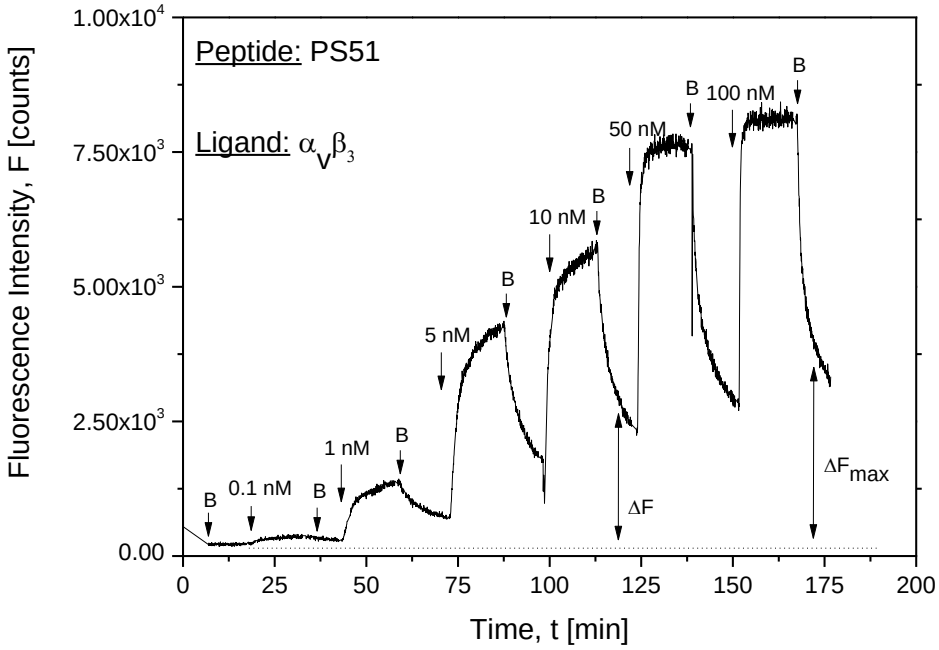

Figure 17: *Scheme of titration assay. A titration of different peptide concentrations is performed by flowing peptide over the surface for 20 minutes per concentration and by rinsing after each concentration with buffer for 10 minutes. Upon binding, an increase in fluorescence intensity is observed. Data points after 10 minutes of rinsing with buffer are used to establish a dose response curve to be fitted with a Langmuir model.*

The fitted dissociation equilibrium constants K_d for integrin $\alpha_V\beta_3$ are summarized in Figure 18 and Table 4. The SPFS analysis revealed that PS48 binds to $\alpha_V\beta_3$ with a K_d of 0.4 nM, similar to the observation on the knottin-TEC205 of K_d=0.6 nM. These results are in line with the ELISA observation shown in the same figure where similarly strong inhibition was measured for both peptides. In addition, the weaker affinity constant of K_d=4.1 was determined for the PS51 which agrees with substantially decreased inhibition in ELISA measurements presented in Table 4. For the negative controls, the binding of clips-TEC213 and TEC218 showed no measurable binding of these peptides to $\alpha_V\beta_3$.

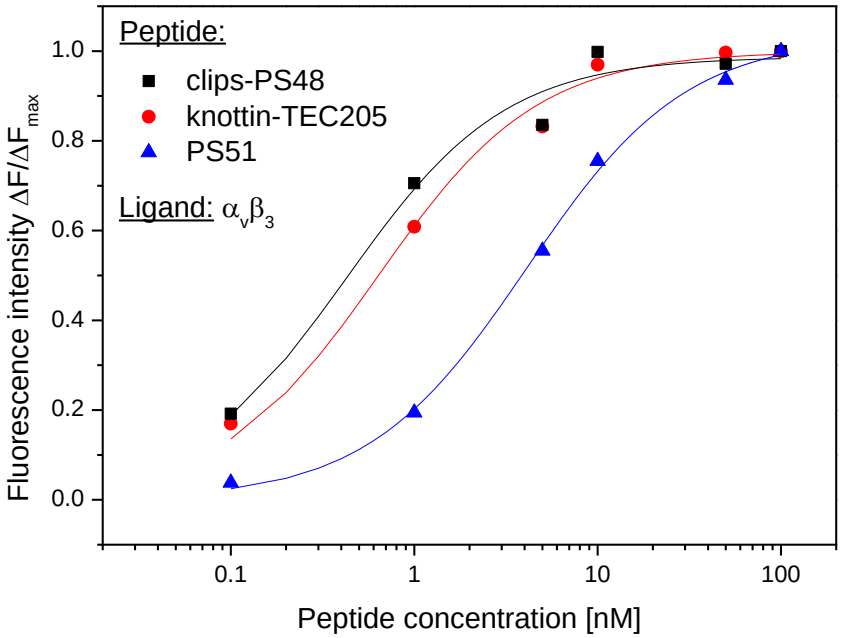

Figure 18: *Fluorescence signal due to the affinity binding of knottin-TEC205, clips-PS48 and PS51 peptides labelled with Cy5 dye to integrin αVβ3 on a thiol-SAM surface. Dots indicate the fluorescence intensity ΔF/ΔFmax for different peptide concentrations. Lines indicate a Langmuir fit.*

Table 4: *Comparison of inhibition rates at 1 µM [%] found by competitive ELISA studies and Kd values [nM] found by SPFS studies for selected peptides and integrin $\alpha_V\beta_3$ on a thiol-SAM surface.*

Peptide	Inhibition at 1 µM [%]	Affinity constant K_d [nM]
clips-PS48	95	0.4
knottin-TEC205	97	0.6
PS51	78	4.1
TEC218	<0	>100
clips-TEC213	<0	>100

The fitted dissociation equilibrium constants K_d for integrin $\alpha_5\beta_1$ are summarized in Figure 19 and Table 5. The analysis of clips-TEC213 with target $\alpha_5\beta_1$ integrin reveals the affinity binding constant of K_d=4.3 nM. For knottin-TEC205 no binding could be determined using a thiol-SAM 2D surface architecture. This observation is contradictory to the findings obtained by inhibition ELISA presented in Table 5 which indicate that biotin labeled knottin RGD binds with higher affinity to $\alpha_5\beta_1$ integrin than clips-TEC213. Additionally, SPFS analysis revealed that the peptides clips-PS48 and TEC218 did not show any binding interaction with the $\alpha_5\beta_1$ integrin. In accordance with results obtained from inhibition assays, also no binding interaction between the $\alpha_5\beta_1$ integrin and PS51 could be observed.

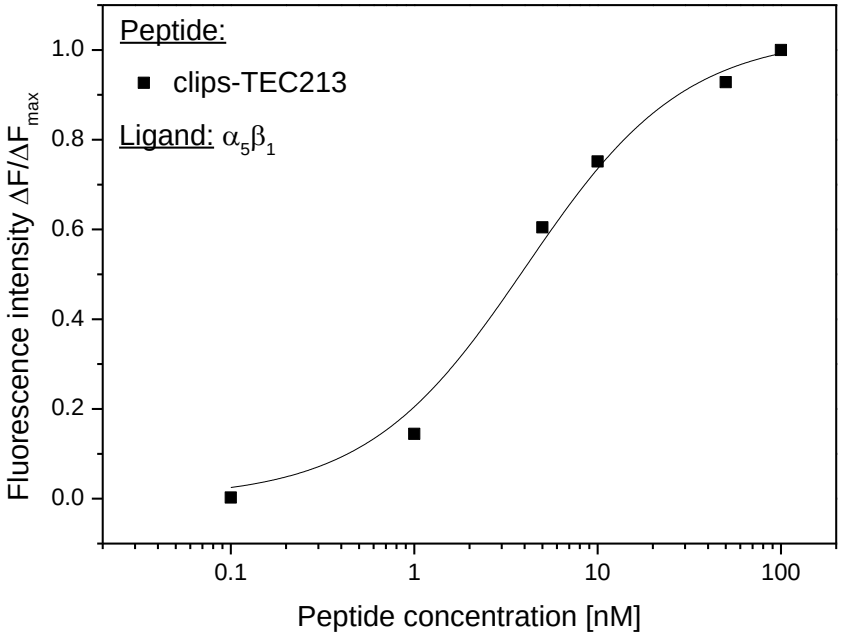

Figure 19: *Fluorescence signal due to the affinity binding of clips-TEC213 labelled with Cy5 dye to integrin $\alpha_5\beta_1$ on a thiol-SAM surface. Dots indicate the fluorescence intensity $\Delta F/\Delta F_{max}$ for different peptide concentrations. Lines indicate a Langmuir fit.*

Table 5: *Comparison of inhibition rates at 1 µM [%] found by competitive ELISA studies and Kd values [nM] found by SPFS studies for selected peptides and integrin $\alpha_5\beta_1$ on a thiol-SAM surface.*

Peptide	Inhibition at 1 µM [%]	Affinity constant K_d [nM]
clips-TEC213	85	4.3
knottin-TEC205	93	>100
PS51	<0	>100
TEC218	<0	>100
clips-PS48	<0	>100

4.2 Peptide Integrin Interaction Study on 3D Surface

In order to improve the accuracy of measuring affinity binding of selected peptides to integrin $\alpha_5\beta_1$ potential quenching effects had to be eliminated. A spacer in form of a pNIPAAM based hydrogel was used for this purpose. This 3D surface architecture is illustrated in Figure 20.

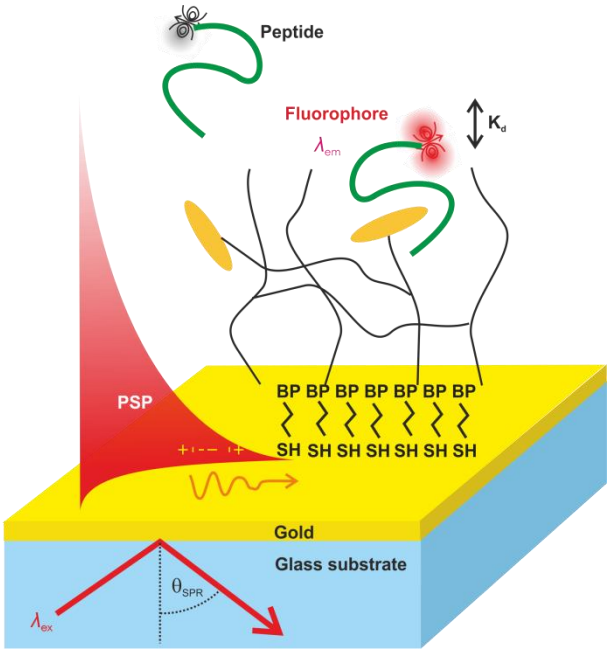

Figure 20: *3D surface architecture based on poly(N)isopropylacrylamide (pNIPAAm) hydrogel binding matrix. In the Kretschmann configuration, a gold film is attached to a glass substrate. For the establishment of a 3D architecture (relying on a thin hydrogel from a pNIPAAM-based polymer), benzophenone (BP) derivatives with thiol- and disulphide anchor groups are chemisorbed onto the gold surface prior to film deposition. Carboxyl groups within methacrylic acid units in the pNIPAAM polymer are used to covalently bind integrin into the hydrogel. Cy5 labelled peptide binds to integrin. The binding is probed at a certain incident angle (θ_{SPR}), at which the light is coupled to electrons in the dielectric interface. Surface plasmons are created and propagate along the surface (therefore called propagating surface plasmons, PSP). The dissociation constant K_d of a peptide binding to immobilized integrin can be investigated.*

Different concentrations and photo-crosslinking densities were investigated to determine the ideal thickness of the hydrogel. Sensor chips were coated with 0.5% w/w and 5% w/w pNIPAAM and photo crosslinked with densities of 2J/cm^2, 4J/cm^2 and 6J/cm^2. SPFS angular scans were made and the thickness of the hydrogel layer was determined using a Winspall simulation (data not shown). Hydrogel layers of 0.5% w/w pNIPAAM, photo crosslinked with 2J/cm^2 , were shown to exhibit a thickness of ~15 nm in dry state and a refractive index of ~1.4, without any buffer flow. In wet state, under constant PBS flow, this hydrogel configuration was shown to exhibit a thickness of ~100 nM and a refractive index of ~1.36 (data not shown). This surface architecture based was used to covalently

immobilize integrin to the surface (Figure 21). A titration of different fluorescently labelled peptide concentrations was performed (***Figure 22***) to obtain a dose response curve to be used for a Langmuir fit to obtain the K_d of integrin-peptide interactions.

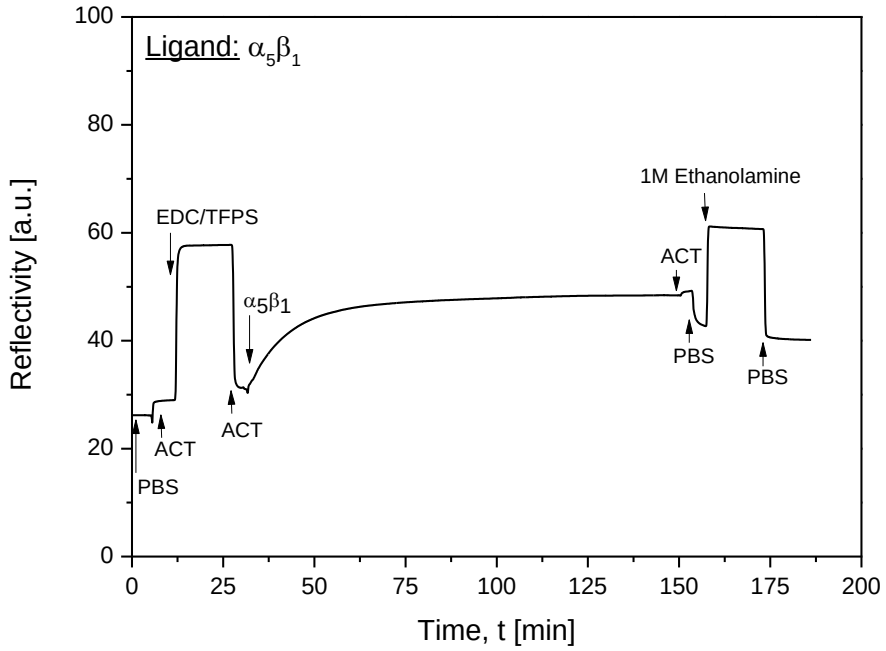

Figure 21: *Sensorgram of immobilization into 3D hydrogel binding matrix. Carboxyl groups of the surface are activated via EDC/TFPS chemistry. Integrin is covalently bound to these groups. Remaining functional groups are blocked with 1 M Ethanolamine. An increase in reflectivity is observed upon binding of molecules to the surface.*

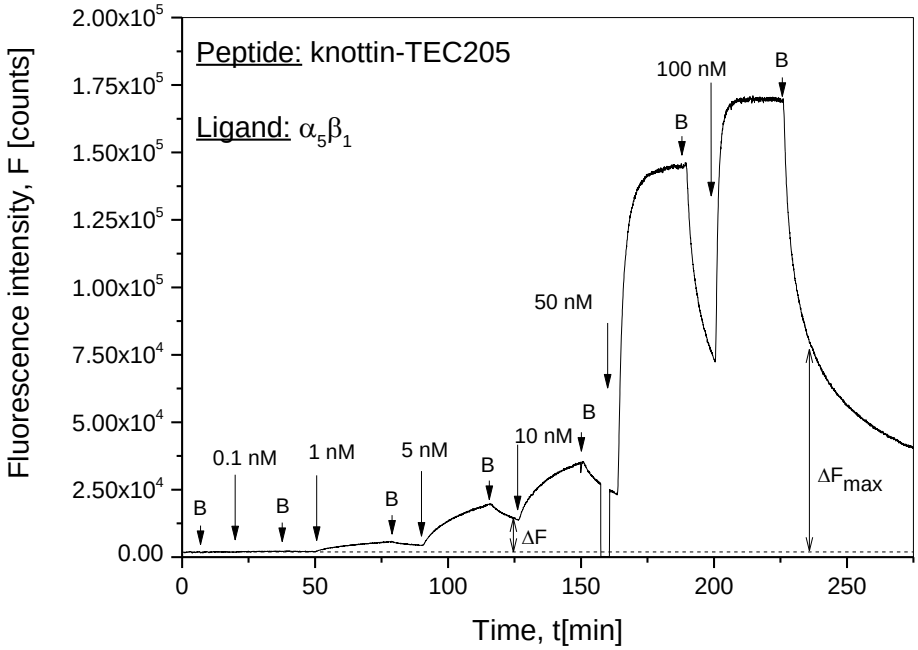

Figure 22: *Scheme of titration assay. A titration of different peptide concentrations is performed by flowing peptide over the surface for 20 minutes per concentration and by rinsing after each concentration with buffer for 10 minutes. Upon binding, an increase in fluorescence intensity is observed. Data points after 10 minutes of rinsing with buffer are used to establish a dose response curve to be fitted with a Langmuir model*

As mentioned earlier, for the integrin $\alpha_5\beta_1$ the fluorescence signal due to the affinity binding of peptides was too weak. In order to reduce the effect of quenching the average distance from the gold surface was increased by using a hydrogel binding matrix with a thickness of about d~100 nm. the fitted dissociation equilibrium constants K_d for integrin $\alpha_5\beta_1$ using a hydrogel binding matrix are summarized in Figure 23 and Table 6. The SPFS analysis revealed that clips-TEC213 binds to $\alpha_5\beta_1$ with K_d of 4.14 ± 0.47 nM, which is lower than the K_d of 8.99 ± 0.36 nM observed for knottin-TEC205. These results are in line with the ELISA observation shown in the same table. In addition, no binding was determined for PS51, which agrees with the ELISA measurements presented in Table 6. For the controls, the binding of clips-PS48 and TEC218 showed no measurable binding of these peptides to $\alpha_5\beta_1$.

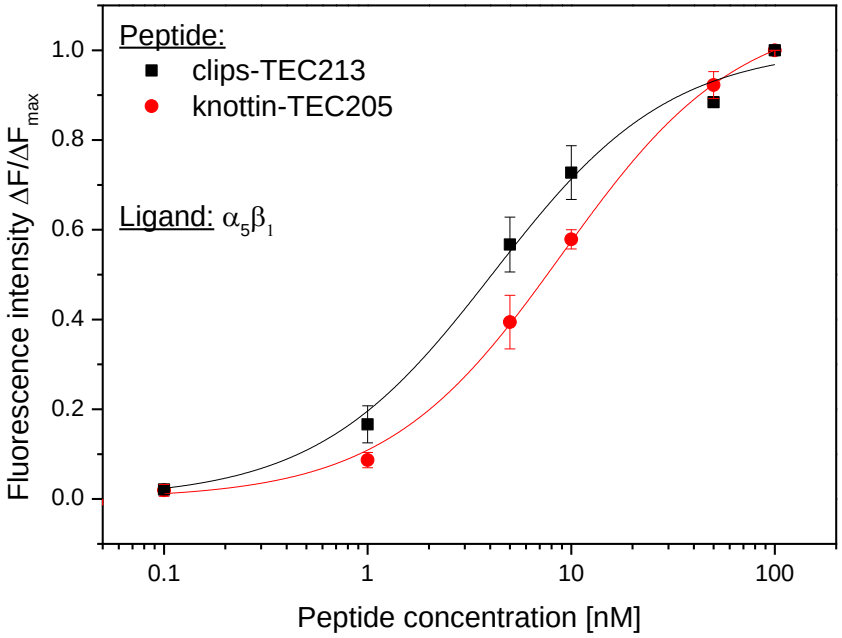

***Figure 23**: Fluorescence signal due to the affinity binding of clips-TEC213 and knottin-TEC205 labelled with Cy5 dye to integrin $\alpha_5\beta_1$ on a pNIPAAm based hydrogel surface. Dots indicate the fluorescence intensity $\Delta F/\Delta F_{max}$ for different peptide concentrations. Lines indicate a Langmuir fit. Errors bars indicate the standard deviation of three independent measurements.*

***Table 6:** Comparison of inhibition rates at 1 µM [%] found by competitive ELISA studies and K_d values [nM] found by SPFS studies for selected peptides and integrin $\alpha_5\beta_1$ on a pNIPAAm based hydrogel surface.*

Peptide	Inhibition at 1 µM [%]	Affinity constant K_d [nM]
clips-TEC213	85	4.14 ± 0.47
knottin-TEC205	93	8.99 ± 0.36
PS51	<0	>100
TEC218	<0	>100
clips-PS48	<0	>100

4.3 Comparison of Surface Architectures

Different surface architectures have been used to investigate the dissociation constant $K_{d.}$ Figure 24 compares the curves measured by using 2D mixed thiol SAM and 3D hydrogel surface architecture. When using a hydrogel surface, the overall fluorescence signal obtained is about 10 times higher compared to the fluorescence signal obtained from using a thiol-SAM surface. This leads to a higher sensitivity of the assay format and a better differentiation between bulk and specific signal. Both bio-interfaces provide consistent titration curves with the dissociation constant determined as Kd=4.2 ± 1.3 nM (error represents the standard deviation) (Figure 25).

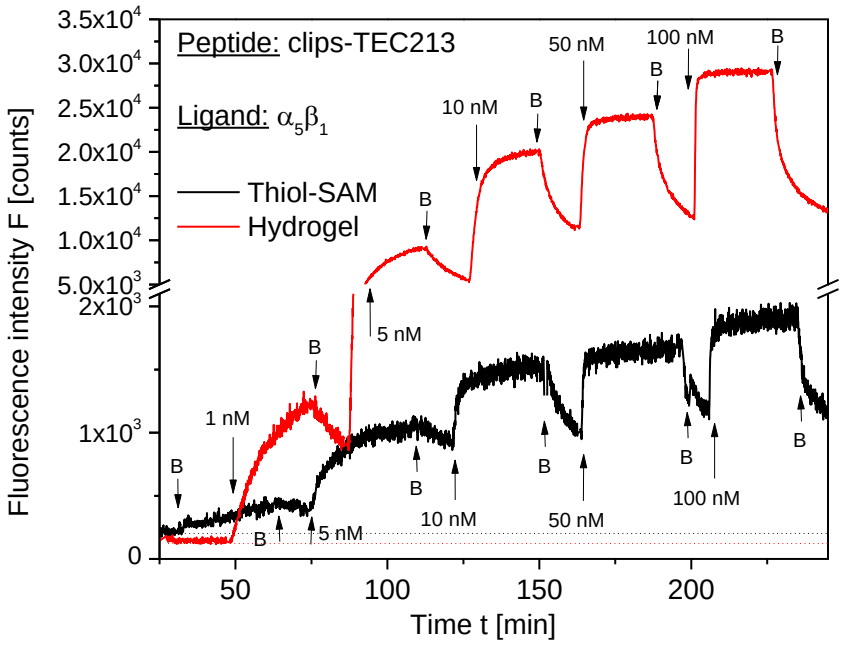

Figure 24: *Scheme of titration assay. A titration of different peptide concentrations is performed by flowing peptide over the surface for 20 minutes per concentration and by rinsing after each concentration with buffer for 10 minutes. Upon binding, an increase in fluorescence intensity is observed. Data points after 10 minutes of rinsing with buffer are used to establish a dose response curve to be fitted with a Langmuir model. A thiol-SAM surface (black) and a hydrogel binding matrix (red) were compared. Overall fluorescence signal observed is higher for the hydrogel binding matrix compared to the thiol-SAM surface.*

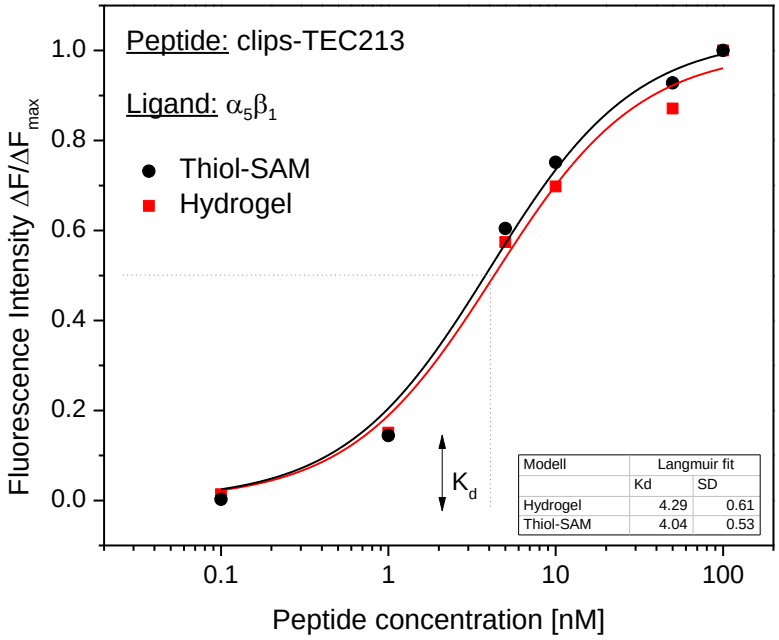

Figure 25: *Fluorescence signal due to the affinity binding of clips-TEC-213 labelled with Cy5 dye to integrin $\alpha_5\beta_1$ on a thiol-SAM surface (black) and in a hydrogel binding matrix (red). The found dissociation constants K_d were the same regardless of surface architecture (4.04 nM for thiol-SAM, 4.29 nM for hydrogel binding matrix). Dots indicate the fluorescence intensity ΔF=ΔFmax for different peptide concentrations. Lines indicate a Langmuir fit.*

4.4 Application of Platform for Click Chemistry-Based Affinity Binding Measurements

The previous part of this Master thesis has focused on biomolecular interaction studies using SPFS in order to measure affinity binding constants. Two different surface architectures were described. These surface architectures can also be implemented into the detection of biomarkers when the assay is flipped around. In that case, peptides will be immobilized on the surface and will serve as ligand. The analyte will be a protein such as an antibody. In this part of the thesis a model system is presented, using CA12 and TP53 peptides as ligand and an anti-CA12 (a-CA12) monoclonal antibody as the ligand to be detected. The goal of this part of the thesis was to establish another coupling chemistry by a click-based coupling protocol.

The click-based coupling protocol was evaluated in a pNIPAAm hydrogel matrix prepared with a thickness in swollen state of ~900 nm and same optical configuration as in previous SPFS studies. Angular fluorescence scans were measured after the incubation of the surface with samples with a-CA12 dissolved at concentration of 10, 100, 1000 ng/mL and reaction with detection antibody a-mIgG (Figure 26).

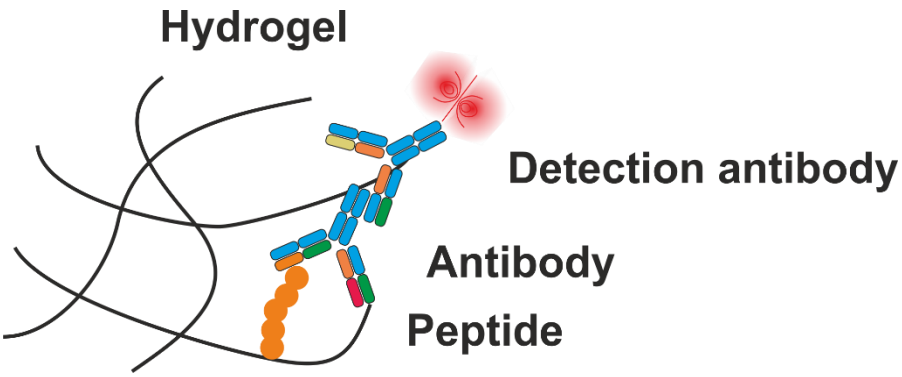

Figure 26: *Scheme of click-based coupling protocol evaluation. A peptide (CA12 or TP53 for control) is clicked into a hydrogel binding matrix. Different concentrations of a peptide-specific antibody (a-CA12) are reacted with the surface and detected with a detection antibody (Alexa Fluor 647 goat anti-mouse IgG).*

Figure 27 shows the acquired angular scan for the hydrogel modified with the specific peptide CA12 where a strong fluorescence peak at the angle θ_{SPR}=47.5 deg is observed (where optical waveguide mode is excited) and no increased fluorescence signal occurs at θ_{SPR}~58 deg (where surface plasmons are excited).

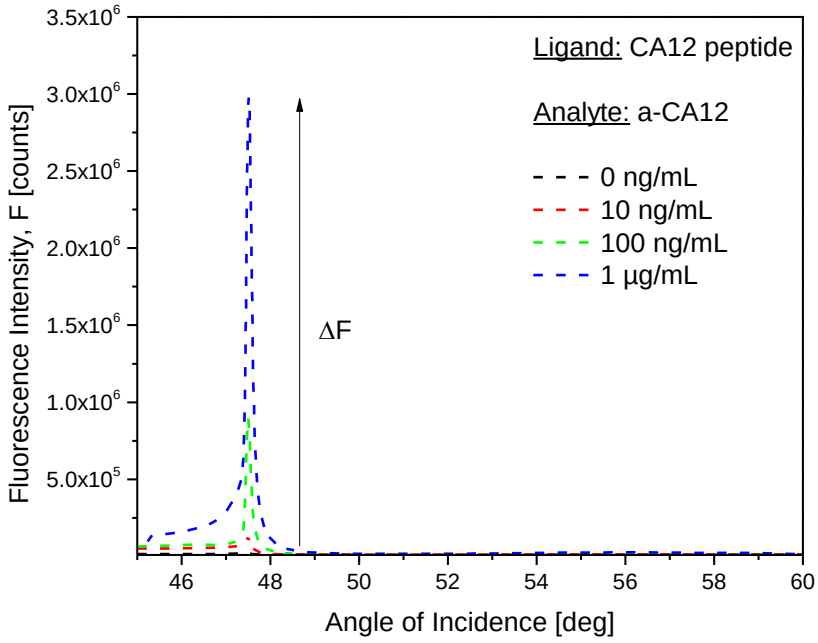

Figure 27: *Angular OWS-enhanced angular scans measured after the sequential analysis of samples with a concentration of a-CA12 of 1,10, 100, and 1000 ng/mL for the hydrogel matrix post-modified with CA12 peptide.*

The specificity of the assay is significantly improved as virtually no response is observed for a hydrogel layer with a reference TP53 peptide immobilized (Figure 28).

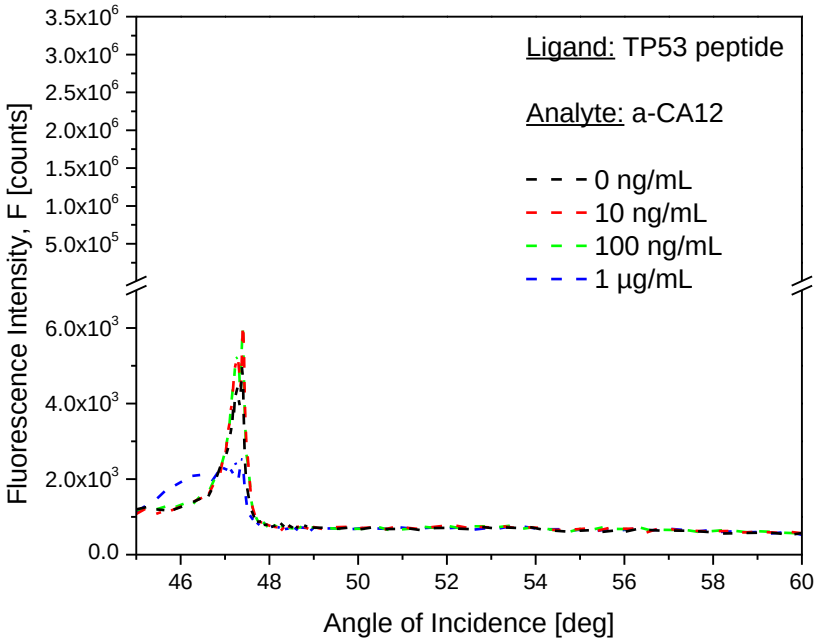

Figure 28: *Angular OWS-enhanced angular scans measured after the sequential analysis of samples with a concentration of a-CA12 of 1,10, 100, and 1000 ng/mL for the hydrogel matrix post-modified with TP53 peptide.*

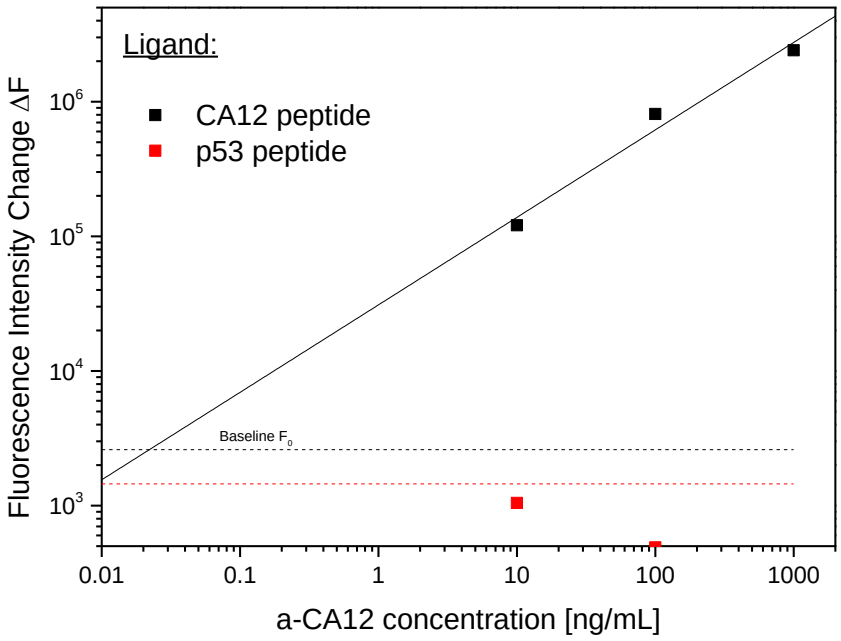

Figure 29: *Comparison of the fluorescence signal increase as a function of a-CA12 concentration.*

5 Discussion

There is a high need for integrin-binders such as peptides for medical purposes. These peptides can be used for cancer imaging or treatment or for the functionalization of synthetic materials to improve cell culturing and regenerative medicine. For the engineering process of such peptides, the evaluation of affinity to integrin is crucial.

In this study we implemented surface plasmon-enhanced spectroscopy (SPFS) to measure the biointeraction of small molecular weight peptides designed for affinity-binding to integrin receptors. Usually, affinity binding can be monitored by a surface plasmon resonance (SPR) biosensor. Here the binding is measured based on induced changes in the refractive index which detune the resonant excitation of surface plasmons. For small molecular weight molecules, the sensitivity of this method is too low due to weak binding induced variations of the refractive index. SPFS represents a method that allows the enhancement of sensitivity. The strength of fluorescence signal originating from the surface is increased and allows the measurement of fluorescence signal kinetics [21]. At our collaborator's laboratory, a high-throughput ELISA platform allowed for successful identification of a panel of cyclic peptides that affinity bind to integrin $\alpha_V\beta_3$ and $\alpha_5\beta_1$. In this platform, the strength of the affinity interaction was determined indirectly in relation to that of a reference knottin-RGD peptide by using a competitive assay format. In order to directly observe the peptide binding to integrin ligands, an optical approach as SPFS was implemented.

We compared the affinity of newly developed bicyclic peptides to already established knottin, cyclic and linear peptides. Firstly, peptide binding was tested for the $\alpha_v\beta_3$ integrin receptor. A thiol-SAM surface was implemented for these measurements with the binding at distances d < 20 nm. It was shown, that the bicylic peptide optimized for this integrin receptor showed the highest affinity compared to other tested peptide structures (K_d=0.4 nM). For a standard knottin peptide a comparable binding constant was observed (K_d=0.6 nM), while for a cyclic peptide a much lower affinity binding (K_d=4.1 nM) was observed. A linear peptide and a bicyclic peptide designed for affinity binding to $\alpha_5\beta_1$ did not show any binding to the $\alpha_v\beta_3$ integrin receptor. When testing the affinity binding of peptides to the $\alpha_5\beta_1$ integrin receptor, the overall fluorescence signal obtained was weak and it was difficult to differentiate between specific binding and bulk changes related to the fluorophore. These issues can be caused by quenching effects that occur when the fluorophore of the peptide interacts with the gold surface. To reduce the effect of quenching the average distance from the gold surface was increased by using a hydrogel binding matrix with a thickness of about d~100 nm. By this method it was possible to measure affinity binding of a bicylic peptide optimized for this integrin receptor (K_d=4.14 ± 0.47 nM). Binding was also observed for the knottin peptide (K_d=8.99 ± 0.36 nM). However, the affinity binding was

much lower compared to the optimized bicycle. For a cyclic, a linear and a bicyclic peptide optimized for $\alpha_v\beta_3$ no affinity binding was observed.

No binding of linear peptides to both tested integrin receptors was observed. The affinity of RGD peptides is affected by steric conformation of the peptide. In linear peptides, the fourth amino acid alters the binding specificity and the binding affinity. Additionally, linear peptides were shown to be highly susceptible to chemical degradation [63]. This could explain why neither in the competition ELISA nor in the SPFS measurements binding was observed. Cyclic peptides can fold into different cyclic structures, influencing the integrin selectivity and affinity [64].

Our study proved that bicyclic peptides are high-affinity integrin-binders and offer a straightforward alternative for established binders such as knottin or cyclic peptides. The dissociation constants observed from SPFS measurements suggest various applications of these integrin-binding peptides. High affinity and selectivity $\alpha_v\beta_3$-binding and $\alpha_5\beta_1$-binding bicyclic peptides could represent a cost-effective alternative to antibodies, for example, in cellular integrin staining, whereas the $\alpha_5\beta_1/\alpha_v\beta_3$-binding bicyclic peptides might be used for applications where non-selective integrin binding is beneficial, for example, in biomaterials. Other possible applications for both $\alpha_v\beta_3$- and $\alpha_5\beta_1/\alpha_v\beta_3$-binding bicycles might be in the field of cancer diagnostics and therapeutics.

When comparing different surface architectures, it was observed that a 2D mixed thiol SAM and 3D hydrogel surface architecture provide consistent titration curves with K_d=4.2 ± 1.3 nM. The overall fluorescence signal obtained when using a hydrogel surface was higher compared to the thiol-SAM surface. Quenching effects are avoided by implementing a hydrogel surface. Both surface architectures were implemented for another assay principle. Here, the assay was flipped around.

In the second part of the project, we established a click-based coupling protocol. Peptides were clicked into a hydrogel binding matrix. The strong peak observed within the SPFS angular scans is due to the amplified fluorescence signal associated with the excitation of optical waveguide mode that confines the energy of excitation at the upper hydrogel interface where the affinity binding occurs. The lack of the signature of the excitation of surface plasmons can be ascribed to the fact that the affinity binding did not occur deep inside the hydrogel due to the short analysis time which did not allow reaching equilibrium. For a hydrogel layer with a reference TP53 peptide immobilized, virtually no response was observed. Therefore, this assay can be considered as very specific. This observation may be ascribed to the improved antifouling properties of the interface which virtually eliminates unspecific sorption of mouse a-CA12 and a-mIgG antibodies.

Additionally, compared to an assay on a thiol-SAM surface, this assay leads to an increased fluorescence signal for the affinity binding of an a-CA12 antibody to a peptide immobilized in a hydrogel binding matrix. This can be ascribed to the enhanced binding capacity of the hydrogel. However, it is important to state that the surface reaction was far from equilibrium and it was likely diffusion limited and thus the sensor response is not proportional to the surface mass density of attached ligands ΔΓ (data not shown). Peptides have been shown to be usable for cancer biomarker detection. Usually, ELISA assays are used to quantitively measure antibody concentrations [65][41]. However, such an assay is only capable of measuring one antibody per time [66]. Microarrays are considered as a promising efficient and sensitive alternative. On one microarray slide, multiple antigens can be spotted, so that many antibodies can then be measured simultaneously, allowing a multiplicity [66]. The amount of antigen printed into one spot is crucial. Different surface architectures improve and increase the number of immobilized antigen, leading to a higher sensitivity. A surface is considered as inadequate if it does not bind the antigen or if the antibody-recognition epitope of the antigen is unavailable (due to antigen orientation on the surface or due to matrix interference, such a surface is inadequate) [67] [68]. Different assays have been reported on using click-chemistry based approaches for biomarker detections [69], [70]. Click chemistry-based coupling protocols provide a powerful tool for biochemical assays and for the bio-conjugation of sensors, when the reaction fulfills all requirements [43], [44].

Literature

[1] P. Mehrotra, “ScienceDirect Biosensors and their applications – A review,” *J. Oral Biol. Craniofacial Res.*, vol. 6, no. 2, pp. 153–159, 2016.

[2] A. Hasan, M. Morshed, A. Paul, A. Polini, T. Kuila, M. Al Hariri, Y. Lee, and A. A. Jaffa, “Recent Advances in Application of Biosensors in Tissue Engineering,” *Biomed Res. Int.*, vol. 2014, pp. 1–18, 2014.

[3] D. Grieshaber, R. MacKenzie, J. Vörös, and E. Reimhult, “Electrochemical Biosensors - Sensor Principles and Architectures,” *Sensors*, vol. 8, no. 12, pp. 1400–1458, 2008.

[4] D. R. The, K. Toth, R. A. Durst, and G. S. Wilson, “Technical report Electrochemical biosensors : recommended definitions and classification,” *Biosens. Bioelectron.*, vol. 16, pp. 121–131, 2001.

[5] S. GS, A. CV, and B. B. Mathew, “Biosensors: A Modern Day Achievement,” *J. Instrum. Technol.*, vol. 2, no. 1, pp. 26–39, 2014.

[6] K. Ramanathan and B. Danielsson, “Principles and applications of thermal biosensors,” *Biosens. Bioelectron.*, vol. 16, no. 6, pp. 417–423, 2001.

[7] R. J. Leatherbarrow and P. R. Edwards, “Analysis of molecular recognition using optical biosensors,” pp. 544–547, 1999.

[8] M. Rusnati and M. Presta, “Cytokine & Growth Factor Reviews Angiogenic growth factors interactome and drug discovery : The contribution of surface plasmon resonance,” *Cytokine Growth Factor Rev.*, 2014.

[9] S. S. Yee, “Surface plasmon resonance sensors: review,” *Sensors and Actuators*, vol. 54, pp. 3–15, 1999.

[10] L. F. Peterson, A. Boyapati, E. Ahn, J. R. Biggs, A. J. Okumura, M. Lo, and M. Yan, “Review article Acute myeloid leukemia with the 8q22 ; 21q22 translocation : secondary mutational events and alternative t (8 ; 21) transcripts,” *Neoplasia*, vol. 110, no. 3, pp. 799–806, 2016.

[11] Y. Yanase, T. Hiragun, K. Ishii, T. Kawaguchi, T. Yanase, M. Kawai, K. Sakamoto, and M. Hide, “Surface Plasmon Resonance for Cell-Based Clinical Diagnosis,” *SENSOR*, vol. 4, pp. 4948–4959, 2014.

[12] F. S. Ligler and C. R. Taitt, “SURFACE PLASMON RESONANCE BIOSENSORS,” in *Optical Biosensors (Second Edition)*, 2008, pp. 185–242.

[13] H. H. Nguyen, J. Park, S. Kang, and M. Kim, “Surface Plasmon Resonance: A Versatile Technique for Biosensor Applications,” *Sensors*, vol. 15, pp. 10481–10510, 2015.

[14] F. E. Ahmed, J. E. Wiley, D. A. Weidner, C. Bonnerup, and H. Mota, “Surface Plasmon Resonance (SPR) Spectrometry as a Tool to Analyze Nucleic Acid – Protein Interactions in Crude Cellular Extracts,” *Cancer Genomics Proteomics*, vol. 310, pp. 303–309, 2010.

[15] J. Bao and S. N. Krylov, “Volatile Kinetic Capillary Electrophoresis for Studies of Protein − Small Molecule Interactions,” *Anal. Chem.*, 2012.

[16] J. W. Attridge, P. B. Daniels, J. K. Deacon, G. a Robinson, and G. P. Davidson, “Sensitivity enhancement of optical immunosensors by the use of a surface plasmon resonance fluoroimmunoassay.,” *Biosens. Bioelectron.*, vol. 6, no. 3, pp. 201–14, 1991.

[17] W. Knoll, M. Zizlsperger, T. Liebermann, S. Arnold, A. Badia, M. Liley, D. Piscevic, F. J. Schmitt, and J. Spinke, “Streptavidin arrays as supramolecular architectures in surface-plasmon optical sensor formats,” *Colloids Surfaces A Physicochem. Eng. Asp.*, vol. 161, no. 1, pp. 115–137, 2000.

[18] Y. Wang, “NEW BIOSENSOR APPLICATIONS OF SURFACE PLASMON AND HYDROGEL OPTICAL WAVEGUIDE SPECTROSCOPY,” Johannes Gutenberg University, Mainz, 2010.

[19] A. Kasry, J. Dostálek, and W. Knoll, “Long- Range Surface Plasmon Enhanced Fluorescence Spectroscopy as a Platform for Biosensors,” 2009.

[20] J. Dostálek and W. Knoll, “Biosensors based on surface plasmon-enhanced fluorescence spectroscopy (Review),” *Biointerphases*, vol. 3, no. 3, p. FD12-FD22, 2008.

[21] S. Hageneder, M. Bauch, and J. Dostalek, “Plasmonically amplified bioassay - Total internal reflection fluorescence vs. epifluorescence geometry,” *Talanta*, vol. 156–157, pp. 225–231, 2016.

[22] W. Knoll, “Biosensors based on surface plasmon-enhanced fluorescence spectroscopy „ Review …,” *Biointerphases*, no. May 2008, pp. 12–22, 2009.

[23] X. Su, Y. Wu, R. Robelek, and W. Knoll, “Surface Plasmon Resonance Spectroscopy and Quartz Crystal Microbalance Study of Streptavidin Film Structure Effects on Biotinylated DNA Assembly and Target DNA Hybridization,” *Langmuir*, vol. 21, no. 14, pp. 348–353, 2005.

[24] D. Yao, F. Yu, J. Kim, J. Scholz, P. E. Nielsen, E. K. Sinner, and W. Knoll, “Surface plasmon field-enhanced fluorescence spectroscopy in PCR product analysis by peptide nucleic acid probes,” *Nucleic Acids Res.*, vol. 32, no. 22, p. e177, 2004.

[25] H. Berney, P. Roseingrave, J. Alderman, W. Lane, and J. K. Collins, “Biosensor surface characterisation : confirming multilayer immobilisation , determining coverage of the biospecies and establishing detection limits,” *Sensors and Actuators*, vol. 44, pp. 341–349, 1997.

[26] G. D. Austin, R. W. J. Watson, and T. D. Amore, “Studies of On-Line Viable Yeast Biomass with a Capacitance Biomass Monitor,” *Biotechnol. Bioeng.*, vol. 43, pp. 337–341, 1994.

[27] J. C. Love, L. A. Estroff, J. K. Kriebel, R. G. Nuzzo, and G. M. Whitesides, *Self-Assembled Monolayers of Thiolates on Metals as a Form of Nanotechnology*. 2005.

[28] M. J. Felipe, N. Estillore, R. B. Pernites, T. Nguyen, R. Ponnapati, and R. C. Advincula, “Interfacial Behavior of OEG À Linear Dendron Monolayers :,” *Langmuir*, pp. 9327–9336, 2011.

[29] C. Vericat, M. E. Vela, G. Benitez, P. Carro, and R. C. Salvarezza, “Self-assembled monolayers of thiols and dithiols on gold : new challenges for a well-known system,” *Chem. Soc. Rev.*, pp. 1805–1834, 2010.

[30] J. Spinke, M. Liley, F. J. Schmitt, H. J. Guder, L. Angermaier, W. Knoll, J. Spinke, M. Liley, and F. Schmitt, “Molecular recognition at selfassembled monolayers : Optimization of surface functionalization Molecular recognition at self-assembled monolayers : Optimization of surface functionalization,” *AIP*, vol. 7012, no. 1993, 2006.

[31] J. J. Gooding, S. Ciampi, and J. J. Gooding, “The molecular level modification of surfaces : from self-assembled monolayers to complex molecular assemblies,” *Chem. Soc. Rev.*, pp. 2704–2718, 2011.

[32] Q. Chai, Y. Jiao, and X. Yu, “Hydrogels for Biomedical Applications: Their Characteristics and the Mechanisms behind Them,” *Gels*, vol. 3, no. 1, p. 6, 2017.

[33] H. G. Schild, “POLY (N-ISOPROPYLACRYLAMIDE): EXPERIMENT , THEORY AND APPLICATION been appearing in the literature with increasing frequency . As Fig . 1 " illustrates , growth has become rather explosive . CH3 CH3,” *Prog. Polym. Sci.*, vol. 17, pp. 163–249, 1992.

[34] M. Toma, U. Jonas, A. Mateescu, W. Knoll, and J. Dostalek, “Active control of SPR by thermoresponsive hydrogels for biosensor applications,” *J. Phys. Chem. C*, vol. 117, no. 22, pp. 11705–11712, 2013.

[35] H. Search, C. Journals, A. Contact, M. Iopscience, and I. P. Address, “Biosensors : recent advances,” *Rep. Prog. Phys.*, vol. 1397, 1997.

[36] P. K. Robinson, “Enzymes : principles and biotechnological applications,” *Assays Biochem.*, vol. 59, pp. 1–41, 2015.

[37] J. P. Chambers, B. P. Arulanandam, L. L. Matta, A. Weis, and J. J. Valdes, “Biosensor Recognition Elements,” pp. 1–12, 2002.

[38] C. Tuerk and L. Gold, “Systematic Evolution of Ligands by Exponential Enrichment : RNA Ligands to Bacteriophage El-T,” *Science (80-.).*, vol. 249, no. 9, pp. 505–510, 1990.

[39] J. W. Ellington, Andrew D.; Szostak, “© 19 90 Nature Publishing Group,” *Nature*, vol. 346, pp. 818–822, 1990.

[40] M. Egholm, O. Buchardt, L. Christensen, C. Behrens, S. M. Freier, D. A. Driver, R. H. Berg, and S. K. Kim, “© 19 9 3 Nature Publishing Group,” *Lett. to Nat.*, vol. 365, pp. 566–568, 1993.

[41] S. K. Vashist, “Comparison of 1-Ethyl-3-(3-Dimethylaminopropyl) Carbodiimide Based Strategies to Crosslink Antibodies on Amine-Functionalized Platforms for Immunodiagnostic Applications,” *diagnostics*, vol. 2, pp. 23–33, 2012.

[42] K. R. Gee, E. A. Archer, and H. C. Kang, “4-Sulfotetrafluorophenyl (STP) esters: New water-soluble amine-reactive reagents for labeling biomolecules,” *Tetrahedron Lett.*, vol. 40, no. 8, pp. 1471–1474, 1999.

[43] H. C. Kolb, M. G. Finn, and K. B. Sharpless, “Click Chemistry: Diverse Chemical Function from a Few Good Reactions,” *Angew. Chemie - Int. Ed.*, vol. 40, no. 11, pp. 2004–2021, 2001.

[44] H. C. Kolb and K. B. Sharpless, “The growing impact of click chemistry on drug discovery,” *DDT*, vol. 8, no. 24, 2003.

[45] L. Liang and D. Astruc, “The copper (I) -catalyzed alkyne-azide cycloaddition (CuAAC) ‘ click ’ reaction and its applications . An overview,” *Coord. Chem. Rev.*, vol. 255, no. 23–24, pp. 2933–2945, 2011.

[46] B. Rolf, “Proceedings of the chemical society,” 1961.

[47] E. Ruoslahti, “RGD AND OTHER RECOGNITION SEQUENCES FOR INTEGRINS,” *Annu. Rev. Cell Dev. Biol.*, vol. 12, pp. 697–715, 1996.

[48] D. Longo, D. Kasper, J. L. Jameson, A. Fauci, S. Hauser, and J. Loscalzo, “Cancer Cell Biology and Angiogenesis,” in *Harrison’s Principles of Internal Medicine*, 2011.

[49] J. S. Desgrosellier and D. A. Cheresh, “Integrins in cancer : therapeutic opportunities,” *Nat. Rev. Cancer*, vol. 10, no. 1, pp. 9–22, 2010.

[50] F. P. Lindberg, R. Armitage, C. Maliszewski, G. Delespesse, and M. Sarfati, “The Vitronectin Receptor and its Associated CD47 Molecule Mediates Proinflammatory Cytokine Synthesis in Human Monocytes by Interaction with Soluble CD23,” *J. Cell Biol.*, vol. 144, no. 4, pp. 767–775, 1999.

[51] S. Kim, K. Bell, S. A. Mousa, and J. A. Varner, “Regulation of Angiogenesis in Vivo by Ligation of Integrin ⌴ 5 ␋ 1 with the Central Cell-Binding Domain of Fibronectin,” *Am. J. Physiol. Cell Physiol.*, vol. 156, no. 4, pp. 1345–1362, 2000.

[52] Z. Chuang, A. Sathirachinda, J. K. Willmann, and S. S. Gambhir, “Detection of Pancreatic Cancer,” *Clic Cancer Res.*, vol. 18, no. 3, pp. 839–849, 2013.

[53] L. Chen, Y. Liu, W. Wang, and K. A. I. Liu, “Effect of integrin receptor ‐ targeted liposomal paclitaxel for hepatocellular carcinoma targeting and therapy,” *Oncol. Lett.*, vol. 10, no. 12, pp. 77–84, 2015.

[54] R. V. Bellamkonda, “Peripheral nerve regeneration : An opinion on channels , scaffolds and anisotropy $,” *Biomaterials*, vol. 27, pp. 3515–3518, 2006.

[55] F. Danhier and A. Le Breton, “RGD-Based Strategies To Target Alpha (v) Beta (3) Integrin in Cancer Therapy and Diagnosis,” *Mol. Pharm.*, vol. 9, no. v, pp. 2961–2973, 2012.

[56] N. Cox, J. R. Kintzing, M. Smith, G. A. Grant, and J. R. Cochran, “Integrin-Targeting Knottin Peptide–Drug Conjugates Are Potent Inhibitors of Tumor Cell Proliferation,” *Angew. Chemie - Int. Ed.*, vol. 55, no. 34, pp. 9894–9897, 2016.

[57] D. Bernhagen, L. De Laporte, and P. Timmerman, “High-Affinity RGD-Knottin Peptide as a New Tool for Rapid Evaluation of the Binding Strength of Unlabeled RGD-Peptides to $\alpha_v\beta_3$, $\alpha_v\beta_5$, and $\alpha_5\beta_1$ Integrin Receptors,” *Anal. Chem.*, vol. 89, no. 11, pp. 5991–5997, 2017.

[58] I. Anac, A. Aulasevich, M. J. N. Junk, P. Jakubowicz, R. F. Roskamp, B. Menges, U. Jonas, and W. Knoll, “Optical characterization of co-nonsolvency effects in thin responsive PNIPAAm-based gel layers exposed to ethanol/water mixtures,” *Macromol. Chem. Phys.*, vol. 211, no. 9, pp. 1018–1025, 2010.

[59] M. J. N. Junk, U. Jonas, and D. Hinderberger, “EPR spectroscopy reveals nanoinhomogeneities in the structure and reactivity of thermoresponsive hydrogels,” *Small*, vol. 4, no. 9, pp. 1485–1493, 2008.

[60] Y. Wang, C. Huang, U. Jonas, T. Wei, J. Dostalek, and W. Knoll, “Biosensors and Bioelectronics Biosensor based on hydrogel optical waveguide spectroscopy,” *Biosens. Bioelectron.*, vol. 25, no. 7, pp. 1663–1668, 2010.

[61] M. Kobayashi, T. Matsumoto, S. Ryuge, K. Yanagita, R. Nagashio, Y. Kawakami, N. Goshima, S. X. Jiang, M. Saegusa, A. Iyoda, Y. Satoh, N. Masuda, and Y. Sato, “CAXII is a sero-diagnostic marker for lung cancer,” *PLoS One*, vol. 7, no. 3, pp. 1–9, 2012.

[62] J. T. Zilfou, S. W. Lowe, A. C. Joerger, A. R. Fersht, M. E. Perry, D. Lane, A. Levine, and X. Lu, “Tumor Suppressive Functions of p53,” *Cold Spring Harb Perspect Biol.*, vol. 1, no. 5, 2014.

[63] S. Liu and W. Lafayette, “Radiolabeled Multimeric Cyclic RGD Peptides as Integrin r,” *Mol. Pharm.*, no. 6, pp. 991–1006, 2006.

[64] K. Temming, R. M. Schiffelers, G. Molema, and R. J. Kok, “RGD-based strategies for selective delivery of therapeutics and imaging agents to the tumour vasculature,” *Drug Resist. Updat.*, vol. 8, pp. 381–402, 2005.

[65] B. K. van Weemen and A. H. W. M. Schuur, “Immunoassay using Antigen-Enzyme Conjugates,” *FEBS Lett.*, vol. 15, no. 3, pp. 232–236, 1971.

[66] Y. Huang and H. Zhu, “Protein Array-based Approaches for Biomarker Discovery in Cancer,” *Genomics. Proteomics Bioinformatics*, no. March, 2017.

[67] K. Zhu, R. Dietrich, A. Didier, D. Doyscher, and E. Märtlbauer, “Recent Developments in Antibody-Based Assays for the Detection of Bacterial Toxins,” *Toxins (Basel).*, vol. 6, pp. 1325–1348, 2014.

[68] S. Seurynch-Servoss, C. L. Baird, K. D. Roland, and R. C. Zangar, “Surface chemistries for antibody microarrays,” *Front. Biosci.*, vol. 12, pp. 3956–3964, 2007.

[69] C. Hart, L. G. Chase, M. Hajivandi, and B. Agnew, “Metabolic Labeling and Click Chemistry Detection Stem Cell Differentiation,” vol. 698, pp. 459–484.

[70] Y. Liu, F. Sato, T. Kawamoto, K. Fujimoto, and S. Morohashi, “Anti-apoptotic effect of the basic helix-loop-helix (bHLH) transcription factor DEC2 in human breast cancer cells,” *Genes to Cells*, vol. 15, pp. 315–325, 2010.

List of figures

List of tables

List of equations

Abbreviations

BP	Benzophenone
BRE	Biorecognition element
CLIPS	Chemical Linkage of Peptides onto Scaffolds
CuAAc	Copper catalysed alkyne azide cycloaddition
EDC	1-Ethyl-3-(3-dimethylaminopropyl)carbodiimide
ECM	Extracellular matrix
TFPS	Sodium para-tetrafluorophenol-sulfonate
k_a	Association rate
k_d	Dissociation rate
K_d	Dissociation constant
LCST	Lower critical solution temperature
MW	Molecular weight
NHS	N-Hydroxysuccinimid
PBS	Phosphate buffered saline
pNIPAAm	Poly(N-isopropylacrylamide)
PSP	Propagating surface plasmon
RGD	Arg-Gly-Asp (arginine-glycine-aspartic acid)
RI	Refractive index
SAM	Self-assembled monolayer
SP	Surface plasmon
SPFS	Surface plasmon-enhanced fluorescence spectroscopy
SPR	Surface plasmon resonance